Copy
RM E54G02

C1

NACA RM E54G02

NACA

RESEARCH MEMORANDUM

PERFORMANCE EVALUATION OF REDUCED-CHORD ROTOR BLADING AS APPLIED TO J73 TWO-STAGE TURBINE

VI - STAGE PERFORMANCE WITH STANDARD ROTOR BLADING AT INLET CONDITIONS OF 35 INCHES OF MERCURY ABSOLUTE AND 700° R

By Elmer H. Davison and Harold J. Schum

Lewis Flight Propulsion Laboratory
Cleveland, Ohio

NATIONAL ADVISORY COMMITTEE
FOR AERONAUTICS

WASHINGTON

July 11, 1957

NACA RM E54G02

NATIONAL ADVISORY COMMITTEE FOR AERONAUTICS

RESEARCH MEMORANDUM

PERFORMANCE EVALUATION OF REDUCED-CHORD ROTOR BLADING AS APPLIED TO J73 TWO-STAGE TURBINE

VI - STAGE PERFORMANCE WITH STANDARD ROTOR BLADING AT INLET CONDITIONS OF 35 INCHES OF MERCURY ABSOLUTE AND 700° R[1]

By Elmer H. Davison and Harold J. Schum

SUMMARY

Stage performance of the J73 turbine was evaluated on the basis of previous performance investigations of the first stages alone and of the two-stage turbines with standard and with reduced-chord rotor blading for a range of rotational speeds and pressure ratios. The results showed that not only both two-stage turbines but also both first-stage turbines had comparable performance. All had wide ranges of efficient operation with peak brake internal efficiencies of over 90 percent. Because of these similarities, this evaluation of stage performance was confined to the standard-bladed two-stage turbine.

Performance of the first stage was correlated with two-stage performance by conducting both investigations at the same turbine-inlet total state and by duplicating the instrumentation behind the first stage. The first stage had a higher work output than the second at over-all pressure ratios less than 2.7; the reverse was true at over-all pressure ratios greater than 3.0. For pressure ratios near design (2.7 to 3.0), both stages yielded nearly equal work at rotor speeds above 60 percent of design equivalent speed. The fact that both turbine stages operated near their peak efficiencies at the design operating point indicated good matching and resulted in good over-all design performance with the two-stage turbine. Furthermore, both stages were well-matched at off-design operating conditions, thereby producing a wide efficient operating range for the two-stage turbine.

INTRODUCTION

The two-stage turbine from the J73 turbojet engine has been investigated at the NACA Lewis laboratory with both standard rotor blading

[1]The information presented herein was previously given limited distribution.

and with reduced-chord rotor blading. The component performance characteristics of both two-stage turbines were determined experimentally at inlet conditions of 35 inches of mercury absolute and 700° R over a range of pressure ratios and equivalent speeds (refs. 1 and 2). Both turbines operated with a brake internal efficiency of over 0.90 at design speed and work output. No significant reduction in turbine performance resulted from using the reduced-chord rotor blades, although a saving of over 40 percent in rotor blade and disk weight was effected.

Because both J73 two-stage turbine configurations operated at efficiencies of over 90 percent at the design operating point and at high efficiencies over a wide range, it was considered of interest to determine the individual stage performance and the stage-matching characteristics. Accordingly, the two turbines were modified, and the first-stage performance with both the standard first-stage rotor and the reduced-chord first-stage rotor was obtained over a range of speeds and pressure ratios. The over-all performance characteristics of the two first-stage turbines are presented in references 3 and 4. The two first-stage turbines also operated at maximum brake internal efficiencies of over 90 percent, both maintaining high efficiencies over wide ranges of stage total-pressure ratio and speed.

Since both two-stage turbines and both first-stage turbines had comparable performance, the stage evaluation presented herein is confined to the standard-bladed turbine investigations and is considered representative of the reduced-chord turbine configuration. The performance of the first-stage turbine was correlated with the performance of the two-stage turbine by conducting both investigations at the same turbine-inlet total state and by duplicating the instrumentation behind the first stage. With this correlation of work output and total-pressure ratio, it was possible to determine the corresponding work output of the second stage and to estimate its efficiency.

SYMBOLS

The following symbols are used in this report:

A	annular area, sq ft
a	local velocity of sound $\sqrt{\gamma g R T}$, ft/sec
c_p	specific heat at constant pressure, Btu/(lb)(°R)
E	enthalpy drop (based on measured torque), Btu/lb
g	gravitational constant, 32.174 ft/sec^2
J	mechanical equivalent of heat, 778 ft-lb/Btu

N rotational speed, rpm

p static pressure, lb/sq ft

p' total pressure, lb/sq ft

p'_x static pressure plus velocity pressure corresponding to axial component of velocity, lb/sq ft

R gas constant, 53.345 ft-lb/(lb)($^\circ$R)

T static temperature, $^\circ$R

T' total temperature, $^\circ$R

V velocity, ft/sec

w weight flow, lb/sec

$\frac{w\sqrt{\theta}}{\delta}\varepsilon$ weight-flow parameter based on equivalent weight flow and equivalent rotor speed

γ ratio of specific heats

δ ratio of inlet-air pressure to NACA standard sea-level pressure, $p'_1/2116$

ε function of $\gamma, \frac{\gamma_0}{\gamma_e}\left[\frac{\left(\frac{\gamma_e+1}{2}\right)^{\frac{\gamma_e}{\gamma_e-1}}}{\left(\frac{\gamma_0+1}{2}\right)^{\frac{\gamma_0}{\gamma_0-1}}}\right]$

η brake internal efficiency, defined as ratio of actual turbine work based on torque measurements to ideal turbine work

θ_{cr} squared ratio of critical velocity to critical velocity at NACA standard sea-level temperature of 518.4° R, $\frac{\frac{2\gamma}{\gamma+1}gRT'}{\frac{2\gamma_0}{\gamma_0+1}gRT'_0}$

ρ static density, lb/cu ft

Subscripts:

cr	critical
d	design
e	engine operating conditions
u	tangential
x	axial
0	NACA standard sea-level conditions
1	turbine-inlet measuring station ahead of first stator
2	turbine measuring station downstream of first stator
3	turbine measuring station 1/8 inch downstream of first rotor
3a	turbine measuring station $2\frac{5}{8}$ inches downstream of first rotor (first-stage turbine)
4	turbine measuring station downstream of second stator
5	turbine-discharge measuring station downstream of second rotor

APPARATUS AND INSTRUMENTATION

Apparatus

The sea-level design conditions as supplied by the engine manufacturer and the design equivalent conditions are as follows:

	Turbine design conditions	Turbine equivalent design conditions
Weight flow, lb/sec	138.7	42.05
Rotational speed, rpm	7950	4041
Inlet temperature, $^{\circ}$R	2060	518.4
Inlet pressure, in. Hg abs	201	29.92

The standard-bladed two-stage turbine from the J73 turbojet engine is described in detail in reference 1. The modifications incorporated into the turbine facility to convert the two-stage unit into the first-stage standard-bladed turbine are explained in reference 3. In both investigations the air to the turbines was supplied by the laboratory combustion air system. This air was metered by a submerged A.S.M.E.

[redacted]

flat-plate orifice and passed through the combustor system where the air was heated. The air was then ducted to the plenum chamber and passed through the turbine proper, finally discharging into the laboratory altitude-exhaust system. Turbine power output was absorbed by two cradled dynamometers of the eddy-current wet-gap type that were connected in tandem. A photograph of the representative over-all turbine setup showing the various turbine components is presented in figure 1.

Instrumentation

The instrumentation employed to determine the over-all performance of the two-stage turbine is described in reference 1 and shown schematically in figure 2(a). The first-stage turbine instrumentation is explained in reference 3 and shown schematically in figure 2(b). In both cases, measurements of total pressure, wall static pressure and total temperature were made at the turbine-inlet measuring station (ahead of first stator) and at the turbine-discharge measuring station (behind last rotor). The instrumentation at the discharge measuring station 3 for the first-stage turbine investigation duplicated the interstage instrumentation present but not reported in the two-stage turbine investigation of reference 1. The instrumentation at station 3 consisted of three Kiel-type total-pressure tubes located at three different radial positions in the flow annular area, a rake of five thermocouples spaced radially at area centers of equal annular areas, and four wall static-pressure taps on both inner and outer walls. The static-pressure taps were spaced 90° apart and the inner and outer pressure taps were diametrically opposed.

The instrumentation at station 3a, $2\frac{1}{2}$ inches downstream of station 3, consisted of five Kiel-type total-pressure tubes, two rakes of five thermocouples each and four static taps on both inner and outer walls. The total-pressure tubes and thermocouples were placed at area centers of equal annular areas, and the static taps were located in the same manner as those at station 3. The total-pressure tubes at station 3a produced more reliable readings than those immediately behind the rotor at station 3 where blade wake interference effects were more prominent. However, when the turbine is rated on the basis of the calculated total pressure $p'_{x,3}$ as in reference 3, the total-pressure measurement at either station 3 or 3a can be used, because the difference in total-pressure measurements has a negligible effect on calculated $p'_{x,3}$.

The total-pressure measurements were not as reliable as the turbine torque and weight-flow measurements. Only a limited number of fixed total-pressure probes could be installed in the turbine. Consequently, complete radial and circumferential pressure variations could not be obtained. Furthermore, the probes were not always alined with the flow direction, because the instruments were fixed while the flow angles

changed with turbine speed and pressure ratio. The error in total-pressure tube reading due to yaw, for most operating conditions, is small, because the shielded total-pressure tubes are insensitive within $\pm 30^{\circ}$ of yaw.

METHODS AND PROCEDURE

Data Correlation

An estimate of the turbine velocity diagrams from the two-stage performance data (ref. 1) at both design and off-design operating conditions indicated that very little exit tangential velocity was present at the exit of the first stage over a wide range of speed and total-pressure ratio. For this reason, the first stage of the two-stage turbine could readily be investigated as an independent unit and the stage performance characteristics evaluated (ref. 3). A similar single-stage investigation of the second stage of the turbine was not conducted, because it was impractical to duplicate inlet flow conditions existing in the two-stage turbine configuration. Consequently, a correlation between actual operating conditions of the first-stage investigation and the two-stage investigation was evolved by use of the duplicated interstage and first-stage instruments.

The first-stage turbine performance presented in this report is based on the data obtained at station 3a (fig. 2(b)) rather than station 3 as used in references 3 and 4. The performance evaluation of the second-stage turbine was also based on the data obtained at station 3a rather than station 3. However, in order to relate the first-stage performance results, it is necessary to utilize the data obtained at the common measuring station 3.

The pertinent correlation data obtained in the investigations reported in references 1 and 3 are presented in figures 3 to 5. The first-stage performance data are shown in figures 3(a), (b), and (c), where, respectively, total-pressure ratios $p_1'/p_{x,3a}'$ and p_1'/p_{3a}' and equivalent work output $E_{1-3}/\theta_{cr,1}$ are plotted against a common abscissa of total-pressure ratio p_1'/p_3' for constant values of percent design equivalent rotational speed. (The ordinate parameters in figures 3 to 5 are multiplied by percent design speed in order to spread the curves.) The two-stage performance data are presented in figure 4, where total-pressure ratio p_1'/p_5' and equivalent work output $E_{1-5}/\theta_{cr,1}$ are plotted against a common abscissa of total-pressure ratio $p_1'/p_{x,5}'$ for constant values of percent design equivalent rotational speed. The data used to correlate the first-stage and two-stage turbine performance are presented in figure 5, which shows the variation of two-stage total-pressure ratio $p_1'/p_{x,5}'$ with first-stage total-pressure ratio p_1'/p_3' for constant values of percent design equivalent rotational speed.

[redacted]

The calculated pressure p_x' is defined as the static pressure behind a rotor plus the velocity pressure corresponding to the axial component of the absolute velocity at the exit of the rotor. This calculated value of turbine-exit stagnation pressure charges the turbine for the energy of the whirl component existing in the exit velocity of the gas. Uniform flow is assumed, which further charges the turbine for the unavailable energy represented by the velocity variations at the turbine exit. This pressure is calculated from the general energy and continuity equations by using the known annulus area at the measuring station and the measured values of weight flow, static pressure, total (stagnation) pressure, and total temperature. The derivation of the equation used to calculate p_x' is given in the appendix.

In order to correlate the data obtained from the first-stage and two-stage turbine investigations, it was necessary to assume that the instruments at measuring station 3 read the same in both investigations. It is assumed that the pressure probes at station 3 read the same when the inlet gas state, rotational speed, and weight flows are identical for both first-stage and two-stage operation. The validity of this assumption is substantiated by observing the variation of the hub and tip values of the static-to-total pressure ratio across the first stator p_2/p_1' with the measured first-stage total-pressure ratio p_1'/p_3' for both the first-stage and two-stage turbines at the design speed (fig. 6). It is readily noted in figure 6 that the two-stage and first-stage data, for all practical purposes, fall on a single curve at both the inner- and outer-turbine shrouds, indicating that the total-pressure probes at the exit of the first-stage rotor read the same whether the second stage is present or not.

Stage Efficiency

Only a brief description of the stage efficiencies calculated will be given here. A more comprehensive discussion is given in the appendix.

First stage. - Two first-stage efficiencies were calculated by the following equations:

$$\eta_{1\text{-}3a} = \frac{E_{1\text{-}3}}{c_p T_1' \left[1 - \left(\frac{p_{3a}'}{p_1'}\right)^{\frac{\gamma-1}{\gamma}}\right]} \tag{1}$$

$$\eta_{1\text{-}3a,x} = \frac{E_{1\text{-}3}}{c_p T_1' \left[1 - \left(\frac{p_{x,3a}'}{p_1'}\right)^{\frac{\gamma-1}{\gamma}}\right]} \tag{2}$$

The ideal first-stage work in equation (1) does not include the energy associated with the exit whirl from that stage, whereas in equation (2) the ideal work does include the energy associated with the exit whirl.

Second stage. - Correspondingly, two second-stage efficiencies were calculated by the following equations:

$$\eta_{3a-5} = \frac{E_{3-5}}{c_p T'_3 \left[1 - \left(\frac{p'_5}{p'_{3a}} \right)^{\frac{\gamma-1}{\gamma}} \right]} \tag{3}$$

$$\eta_{3a-5,x} = \frac{E_{3-5}}{c_p T'_3 \left[1 - \left(\frac{p'_{x,5}}{p'_{3a}} \right)^{\frac{\gamma-1}{\gamma}} \right]} \tag{4}$$

The ideal second-stage work in equation (3) includes the entrance (first-stage exit) whirl energy but does not include the second-stage exit whirl energy. The ideal second-stage work in equation (4) includes both the entrance (first-stage exit) whirl energy and the second-stage exit whirl energy.

3194

RESULTS AND DISCUSSION

The performance of a multistage turbine is closely related to the manner in which blade-row choking is affected by over-all pressure ratio and rotational speed. Therefore, the results are discussed under three separate headings: Blade-Row Choking, Stage Performance, and Stage Matching. The performance results presented herein for the first-stage turbine differ slightly from those in reference 3, because the performance is based on data obtained at station 3a rather than at station 3.

Blade-Row Choking

Figure 5 shows that, for any given rotational speed (60 percent of design or above), the first-stage pressure ratio p'_1/p'_3 increases with increasing two-stage over-all pressure ratio $p'_1/p'_{x,5}$ up to some value and then remains constant with any further increase in over-all pressure ratio. The value at which the first-stage pressure ratio remains constant increases with increasing rotational speed up to 110 percent of design and then decreases as speed increases from 110 to 130 percent.

Although it is not apparent from figure 5, because the ordinate has been multiplied by a speed ratio, the data showed that the first-stage pressure ratio p_1'/p_3' became constant for all speeds above 60 percent of design for two-stage pressure ratios above 3.2. It should be noted, however, that the value at which the first-stage pressure ratio became constant varied with rotational speed. This variation in first-stage pressure ratio shows that choking is occurring in either the second stator or rotor or both. Choking in the second stage of the two-stage turbine occurs for a given speed at two-stage pressure-ratio values greater than the value at which the first-stage pressure ratio first becomes constant.

When the first stage is operating as a component of the two-stage turbine at design speed, neither the first-stage rotor nor the first-stage stator is choked (fig. 6). The rotor of the first stage is not choked during two-stage operation, since the static-to-total pressure ratio at the first-stator exit can be lowered when the first stage is operated as an independent unit. Evidence that the first stator is not choked is obtained from this figure, since the static-to-total pressure ratio at the stator exit never reached a choking value when the first stage was operating as a component of the two-stage turbine. Thus, at design speed it can be concluded that choking in the turbine occurs only downstream of the first stage for two-stage operation.

Figure 7 was constructed in order to determine which blade row in the second stage was choking at design speed. Figures 7(a) and (b) show the static-pressure variation through the two-stage turbine with over-all pressure ratio $p_1'/p_{x,5}'$ at the design speed as measured at the outer and inner casings, respectively. Choking in a blade row, or downstream of the blade row, is indicated when the ratio of static to inlet total pressure p/p_1' ahead of the blade row remains constant with increasing over-all pressure ratio $p_1'/p_{x,5}'$. Choking in a given blade row rather than some point downstream of the blade row occurs if the pressure-ratio curve ahead of the blade row levels out at a lower over-all pressure ratio than those curves at measuring stations farther downstream.

Examination of the static-pressure variation through the turbine (fig. 7) indicates that the second rotor is completely choked for over-all pressure ratios greater than approximately 3.2. Consequently, there is no static-pressure variation at any upstream measuring station for over-all pressure ratios greater than 3.2. The rate of change of the static pressure at station 3 (ahead of the second stator) as an over-all pressure ratio of 3.2 is approached is less than that of station 4 (ahead of the second rotor), which indicates that the second stator probably chokes almost simultaneously with the second rotor. The magnitude of the static-to-total pressure ratio across the first stator and rotor is not

sufficient to choke either the first-stage stator or rotor, as was also evident from figure 6, which showed that with the second stage removed much lower static-to-total pressure ratios were obtained at station 2 before the first rotor choked. It can be concluded, then, that the second-stage rotor of the J73 two-stage standard-bladed turbine definitely chokes at over-all pressure ratios greater than 3.2 at the design speed. Furthermore, it is probable that the second-stage-stator blade row chokes almost simultaneously.

Stage Performance

Stage work. - The variation of the first- and second-stage work with over-all turbine pressure ratio $p_1'/p_{x,5}'$ for various values of percent design equivalent rotational speed is shown in figure 8, which was obtained by cross-plotting the data from figures 3(c), 4(b), 4(c), and 5.

Figure 8 shows that, at turbine speeds of 60 percent of the design speed and above, the equivalent-shaft-work outputs $E/\theta_{cr,1}$ of the two stages are approximately equal for over-all pressure ratios $p_1'/p_{x,5}'$ between 2.7 and 3.0. Design equivalent work (28.48 Btu/lb) was obtained at an over-all pressure ratio of approximately 2.75 and design equivalent speed for the two-stage turbine, as reported in reference 1. At all speeds, it was found that the first stage of the turbine produced more than half the total work output of the two-stage turbine at over-all pressure ratios less than 2.7; whereas, the second stage yielded more work at over-all pressure ratios greater than 3.0. For turbine speeds of 60 percent of design and above, the work output of the first stage increased with over-all pressure ratio $p_1'/p_{x,5}'$ up to some value of over-all pressure ratio and then remained constant. The value of over-all pressure ratio at which the first-stage work output leveled-off increased from 2.8 for 60-percent design speed to about 3.2 for 130-percent design speed. This leveling-off of first-stage work output results because the second stage is choked at the higher over-all pressure ratios. In contrast, the second-stage work output increased continuously with over-all pressure ratio. At over-all pressure ratios above 3.2, the first-stage work output reached a maximum between 100 and 110 percent of design speed, while the second-stage work output increased continuously with speed. The stage work division for 20- and 40-percent design speed is also included in figure 8, although the work division at pressure ratios higher than 2.0 and 2.2 for 20- and 40-percent design speed, respectively, was not obtained in the investigation.

Stage efficiency. - The variation of stage efficiency with turbine over-all pressure ratio $p_1'/p_{x,5}'$ for various values of percent equivalent design rotational speed is shown in figure 9. These efficiencies were calculated with equations (1) to (4) and data from figures 3 to 5. Both second-stage efficiencies shown in figure 9 assume that the second-stage stator utilizes the whirl at the exit of the first stage. The efficiency η_{3a-5}, based on measured total pressure p_5', is less reliable than the efficiency $\eta_{3a-5,x}$ based on the calculated total pressure $p_{x,5}'$, because small errors in measured total pressure are magnified in the efficiency calculation. However, the efficiency η_{3a-5} is quite useful in determining the order of magnitude of the exit-whirl energy from the second stage and in determining how the magnitude of this energy varies with pressure ratio and speed. The efficiency $\eta_{3a-5,x}$ has the most significance when turbine performance is related to

engine performance, because the exit-whirl energy from the second stage is not useful thrust-producing energy. In comparing the aerodynamic performance of the first and second stages, the efficiencies based on measured total pressures are most useful.

If the first-stage efficiency is considered (fig. 9), it will be noted that at low speeds maximum efficiency is obtained at low over-all pressure ratios, while the reverse is true at high speeds. Between 80 and 110 percent of design speed, there is little variation in first-stage efficiency η_{1-3a} over most of the pressure-ratio range. At speeds greater or less than this range, the variation of efficiency with pressure ratio becomes much more pronounced. The level of first-stage efficiency η_{1-3a} over most of the pressure-ratio range reaches a maximum at design speed. The difference between the two first-stage efficiencies shown decreases to a minimum at 120 percent of design speed and then increases when the speed is increased to 130 percent of design. This difference between efficiencies is indicative of the amount of whirl at the exit of the first stage. It can be noted from figures 8 and 9 that the first-stage work output, in one respect, essentially parallels the efficiency variation observed, in that maximum first-stage work and maximum first-stage efficiency occurred at about 100 percent of design speed.

The second-stage efficiency $\eta_{3a-5,x}$ (fig. 9) decreases with increasing over-all pressure ratio for the 60 and 70 percent of design speed conditions. At speeds above 70 percent the efficiency peaks at some pressure ratio for a given speed. In general, this peak or maximum efficiency increases and occurs at increasingly higher pressure ratio with increasing speed. For 70-percent speed and above, comparison of efficiencies η_{3a-5} and $\eta_{3a-5,x}$ shows that the difference between the efficiencies decreases with increasing pressure ratio to a minimum and then increases with further increases in pressure ratio. This results because the whirl at the exit of the second stage changes from positive values at low pressure ratio to negative values at high pressure ratio. The whirl velocity at the exit of the turbine is probably zero at some pressure ratio (near maximum $\eta_{3a-5,x}$), and at this pressure ratio the two efficiencies η_{3a-5} and $\eta_{3a-5,x}$ should theoretically have the same value. That this is not the case for the efficiencies shown in figure 9 can be attributed mainly to the error in total-pressure measurements and the manner in which the total pressure $p'_{x,5}$ is calculated. For the 60-percent speed case presented, the speed and pressure ratios were such that the exit whirl was always negative. The efficiencies over the limited range of pressure ratio for 20- and 40-percent speed are also included in figure 9.

Figure 10 shows the effect of rotational speed on the second-stage efficiency $\eta_{3a-5,x}$. In general, the peak efficiency, at and above 80 percent of the design equivalent speed, increases with increasing speed. Reference 5 demonstrates analytically that increasing blade speed for a choked turbine tends to reduce the relative inlet Mach numbers to the rotor and improve the reaction across the rotor. The increase in peak efficiency of the second stage with increasing speed is attributed to these effects. The low efficiencies obtained in this stage at low pressure ratio and high speed can be attributed to the windmilling effect of the last stage under these operating conditions. At low speeds (60 and 70 percent of design) the energy of the exit whirl is appreciable compared with the work output of the second stage.

Stage Matching

The over-all performance of the standard-bladed two-stage turbine is shown in figure 11 (reproduced from ref. 2), where the performance is based on the over-all two-stage turbine pressure ratio $p'_1/p'_{x,5}$. The two-stage performance was characterized by a high efficiency over a broad range of operation.

Increasing the over-all pressure ratio $p'_1/p'_{x,5}$ above 2.0 affected the flow conditions in the first stage to a much smaller extent than in the second stage. The performance of the first stage is affected primarily by changes in rotational speed. Operation of the first-stage turbine as part of the two-stage turbine is analogous to operating along a line of constant low pressure ratio in figure 11. Thus, the work output and efficiency (η_{1-3a}) of the first-stage increased with rotational speed to maximum values and then decreased with further increases of speed.

3194

In contrast to first-stage operation, both over-all pressure ratio and blade speed have a pronounced effect on the second-stage operation. Operation of the second stage at constant rotational speed is analogous to operating over the whole range of pressure ratio along a constant-speed line in figure 11. For the same two-stage operating conditions, the first stage operates over a much more restricted range of pressure ratio. Thus, at all speeds, the second-stage work output increases continuously with increasing over-all pressure ratio. The efficiency ($\eta_{3a-5,x}$) peaks at some over-all pressure ratio for equivalent speeds between 80 and 120 percent of design. At the lower speeds, the exit whirl is nearly always negative and increases with over-all pressure ratio. For higher speeds the exit whirl is nearly always positive and decreases with over-all pressure ratio. Thus, the second-stage efficiency $\eta_{3a-5,x}$ continually decreases with increasing over-all pressure ratio for the low-speed range and increases for the high-speed range.

At the design operating condition (over-all pressure ratio of 2.75, 100-percent design speed), the two stages of the turbine were well matched. Both stages had nearly equal work outputs, the first stage was operating near maximum efficiency, and the second stage was operating near maximum efficiency for the 100-percent design speed condition. In addition, the tangential component of velocity at the exit of the second stage was small at the design operating condition.

The matching characteristics of the two stages were such that good performance was obtained over a broad range of operating conditions as well as at the design point. Good performance at the low speed, low over-all pressure-ratio condition resulted because the first stage maintained a high efficiency while producing the major portion of the

over-all work output. At the higher speeds and over-all pressure ratios, the first stage maintained a high level of efficiency and work output, while the second stage produced the major portion of the over-all work output at a high efficiency.

Although the preceding discussion is limited to the results obtained for the standard-bladed turbine configuration, the same general characteristics are believed to exist for the reduced-chord turbine configuration, inasmuch as both first-stage and two-stage turbine configurations yielded comparable performance characteristics.

3194

SUMMARY OF RESULTS

From a stage-performance analysis of the standard-bladed J73 two-stage turbine, the following results were obtained:

1. At over-all total-pressure ratios between 2.7 and 3.0, nearly equal work distribution for the two turbine stages prevailed at all equivalent speeds above 60 percent of design.

2. At all speeds, the first stage of the turbine produced more than half the total work output of the two-stage turbine at over-all pressure ratios less than 2.7, whereas the second stage yielded more work at over-all pressure ratios greater than 3.0.

3. For turbine speeds of 60 percent of design and above, the work output of the first stage leveled-off with increasing over-all pressure ratio at a pressure ratio that increased from 2.8 at 60-percent design speed to 3.2 at 130-percent design speed. In contrast, the second-stage work output increased continuously with over-all pressure ratio. At over-all pressure ratios above 3.2, the first-stage work output reached a maximum between 100 and 110 percent of design speed, while the second-stage work output increased continuously with speed.

4. Increasing the over-all pressure above 2.0 affected the flow conditions in the first stage of the two-stage turbine to a much smaller extent than in the second stage. The performance of the first stage was affected primarily by changes in rotational speed. Maximum first-stage efficiency was obtained at design speed.

5. At and above 80 percent of the design equivalent speed, the second-stage efficiency peaked at some over-all pressure ratio. In general, this peak or maximum efficiency increased and occurred at increasingly higher pressure ratios as the speed was increased. At speeds between 80 and 120 percent of design, the whirl at the exit of the second stage changed from positive values at low pressure ratios to negative values at high pressure ratios. At the lower speeds, the exit whirl was

nearly always negative and increased with increasing over-all pressure ratio. For higher speeds, the exit whirl was nearly always positive and decreased with increasing over-all pressure ratio. Thus, the second-stage efficiency continually decreased with increasing over-all pressure ratio for the low speed range and increased for the high speed range.

6. At the design operating condition the two stages of the turbine were well matched. Both stages had nearly equal work outputs, the first stage was operating near maximum efficiency, and the second stage was operating near maximum efficiency for the 100-percent design speed condition. In addition, the tangential component of velocity at the exit of the second stage was small at the design operating condition.

3194

7. The two turbine stages were well matched at off-design operating conditions, giving the two-stage turbine a wide range of efficient operation. Good performance at the low speed, low over-all pressure-ratio condition resulted because the first stage maintained a high efficiency while producing the major portion of the over-all work output. At the higher speeds and over-all pressure ratios, the first stage maintained a high level of efficiency and work output while the second stage produced the major portion of the over-all work output at a high efficiency.

8. The second-stage rotor of the two-stage turbine choked at over-all pressure ratios greater than 3.2 at the design equivalent speed.

Lewis Flight Propulsion Laboratory
National Advisory Committee for Aeronautics
Cleveland, Ohio, July 7, 1954

[redacted]

APPENDIX - DERIVATION OF TOTAL-PRESSURE AND EFFICIENCY EQUATIONS

Total Pressure

The equation for calculating the total pressure p_x' based on the axial component of velocity at the turbine exit can be derived from a combination of the following equations:
Continuity:

$$w = \rho A V_x \tag{A1}$$

State:

$$p = \rho R T \tag{A2}$$

Energy:

$$\frac{T'}{T} = 1 + \frac{\gamma - 1}{2}\left(\frac{V}{a}\right)^2 \tag{A3}$$

Isentropic relations:

$$\frac{p'}{p} = \left(\frac{T'}{T}\right)^{\frac{\gamma}{\gamma-1}} \tag{A4}$$

Combining equations (A1), (A2), and (A4) gives an equation for the axial velocity:

$$V_x = \frac{w}{A}\frac{RT'}{p'}\left(\frac{p'}{p}\right)^{\frac{1}{\gamma}} \tag{A5}$$

This velocity is used in the energy equation to calculate p_x', neglecting the tangential component of velocity at the turbine exit. From equations (A3) and (A4)

$$p_x' = p\left[1 + \frac{\gamma - 1}{2\gamma g R}\frac{V_x^2}{T'}\left(\frac{p'}{p}\right)^{\frac{\gamma-1}{\gamma}}\right]^{\frac{\gamma}{\gamma-1}} \tag{A6}$$

The total pressure p_x' at the turbine exit can be calculated from equations (A5) and (A6) from the known values of w, A, p, p', and T'. The kinetic energy contained in the exit tangential velocity component is considered a loss when the turbine efficiency is based on the exit total pressure p_x'.

Stage Efficiency

A number of stage efficiencies can be calculated for the expansion process obtained in the two-stage turbine. The value of the stage efficiency calculated depends on the definition of ideal enthalpy change. Figure 12 is a temperature-entropy diagram depicting the expansion process in the two-stage turbine.

First stage. - In the first-stage expansion process between stations 1 and 3 the ideal enthalpy change could be defined as the difference (fig. 12) between the enthalpy value at the entrance total temperature T_1' and any one of the three ideal exit temperatures at station 3. The differences between the ideal exit temperatures are a function of the magnitude of the kinetic energy of the gas at the exit of the first stage. This exit kinetic energy is separated in figure 12 into the kinetic energy $(V_x^2/2gJ)_3$ of the axial component of velocity and the kinetic energy $(V_u^2/2gJ)_3$ of the tangential component of velocity. Since all this kinetic energy can be utilized to produce work in the second stage of the turbine, the ideal enthalpy change in the first stage should be based on ideal total temperature $(T_3')_I$. For an ideal enthalpy change based on ideal exit total temperature $(T_3')_I$, the first-stage efficiency is calculated as follows:

$$\eta_{1\text{-}3a} = \frac{c_p(T_1' - T_3')}{c_p\left[T_1' - (T_3')_I\right]} = \frac{c_p(T_1' - T_3')}{c_pT_1'\left[1 - \left(\frac{p_{3a}'}{p_1'}\right)^{\frac{\gamma-1}{\gamma}}\right]} \tag{A7}$$

Another useful first-stage efficiency was determined based on the ideal exit total temperature $(T_3')_{II}$, as follows:

$$\eta_{1\text{-}3a,x} = \frac{c_p(T_1' - T_3')}{c_p\left[T_1' - (T_3')_{II}\right]} = \frac{c_p(T_1' - T_3')}{c_pT_1'\left[1 - \left(\frac{p_{3a,x}'}{p_1'}\right)^{\frac{\gamma-1}{\gamma}}\right]} \tag{A8}$$

In using equation (A8) to rate the first stage, the kinetic energy contained in the exit tangential velocity component is considered a loss. A comparison of the efficiency obtained by equation (A8) with that obtained by equation (A7) is useful in determining the amount of whirl energy at the exit of the first stage.

[redacted]

Second stage. - The kinetic energy at the exit of the first stage can be utilized to produce work by the second stage. Therefore, the state of the gas entering the second stage is assumed for purposes of rating the second stage to be defined by the total temperature T'_3 and the total pressure p'_{3a}.

In the second-stage expansion process between stations 3 and 5, the ideal enthalpy change could be defined as the difference (fig. 12) between the enthalpy value at the entrance total temperature T'_3 and any one of the three ideal exit temperatures at station 5. As at station 3, the differences between the ideal exit temperatures at station 5 are a function of the magnitude of the kinetic energy of the gas at the exit of the second stage. This exit kinetic energy was again separated into the kinetic energy of the axial component of velocity $(V_x^2/2gJ)_5$ and the kinetic energy of the tangential component of velocity $(V_u^2/2gJ)_5$. In a stationary turbine, this exit kinetic energy could not be utilized, and the ideal enthalpy change would therefore be based on exit temperature $(T_5)_{III}$. However, for a turbojet engine, part or all of this exit kinetic energy can be used to develop a useful propulsive force and should not be charged to the turbine as a loss. The exit kinetic energy $(V_u^2/2gJ)_5$ of the tangential component of velocity is not normally available as useful thrust-producing energy. The ideal enthalpy change across the second stage should therefore be based on the ideal exit temperature $(T'_5)_{II}$. For an ideal enthalpy change based on ideal exit total temperature $(T'_5)_{II}$, the second-stage efficiency is calculated as follows:

$$\eta_{3a-5,x} = \frac{c_p(T'_3 - T'_5)}{c_p\left[T'_3 - (T'_5)_{II}\right]} = \frac{c_p(T'_3 - T'_5)}{c_pT'_3\left[1 - \left(\frac{p'_{x,5}}{p'_3}\right)^{\frac{\gamma-1}{\gamma}}\right]} \qquad (A9)$$

In using equation (A9) to rate the second stage, the kinetic energy contained in the exit tangential velocity component is considered a loss.

Another useful second-stage efficiency was determined based on the ideal exit total temperature $(T'_5)_I$, as follows:

$$\eta_{3a-5} = \frac{c_p(T'_3 - T'_5)}{c_p\left[T'_3 - (T'_5)_I\right]} = \frac{c_p(T'_3 - T'_5)}{c_pT'_3\left[1 - \left(\frac{p'_5}{p'_3}\right)^{\frac{\gamma-1}{\gamma}}\right]} . \qquad (A10)$$

This efficiency serves two useful purposes: It is a measure of the aerodynamic performance of the second stage; and, when it is compared with the efficiency obtained by equation (A9), the amount of energy in the exit whirl can be determined.

Ratings of the turbine stages in the investigation reported herein were based on actual enthalpy changes obtained from the dynamometer torque measurements rather than on measured total temperatures T_3' and T_5' as in equations (A7) to (A10). The efficiency equations based on dynamometer torque are given in the METHODS AND PROCEDURE section of this report.

3194

REFERENCES

1. Berkey, William E., Rebeske, John J., Jr., and Forrette, Robert E.: Performance Evaluation of Reduced-Chord Rotor Blading as Applied to J73 Two-Stage Turbine. I - Over-All Performance with Standard Rotor Blading at Inlet Conditions of 35 Inches of Mercury Absolute and 700° R. NACA RM E52G31, 1957.

2. Schum, Harold J., Rebeske, John J., Jr., and Forrette, Robert E.: Performance Evaluation of Reduced-Chord Rotor Blading as Applied to J73 Two-Stage Turbine. II - Over-All Performance at Inlet Conditions of 35 Inches of Mercury Absolute and 700° R. NACA RM E53B25, 1957.

3. Schum, Harold J.: Performance Evaluation of Reduced-Chord Rotor Blading as Applied to J73 Two-Stage Turbine. III - Over-All Performance of First-Stage Turbine with Standard Rotor Blades at Inlet Conditions of 35 Inches of Mercury Absolute and 700° R. NACA RM E53L28a, 1957.

4. Schum, Harold J.: Performance Evaluation of Reduced-Chord Rotor Blading as Applied to J73 Two-Stage Turbine. IV - Over-All Performance of First-Stage Turbine with Reduced-Chord Rotor Blades at Inlet Conditions of 35 Inches of Mercury Absolute and 700° R. NACA RM E53L29, 1957.

5. English, Robert E., and Cavicchi, Richard H.: One-Dimensional Analysis of Choked-Flow Turbines. NACA Rep. 1127, 1953. (Supersedes TN 2810.)

[redacted]

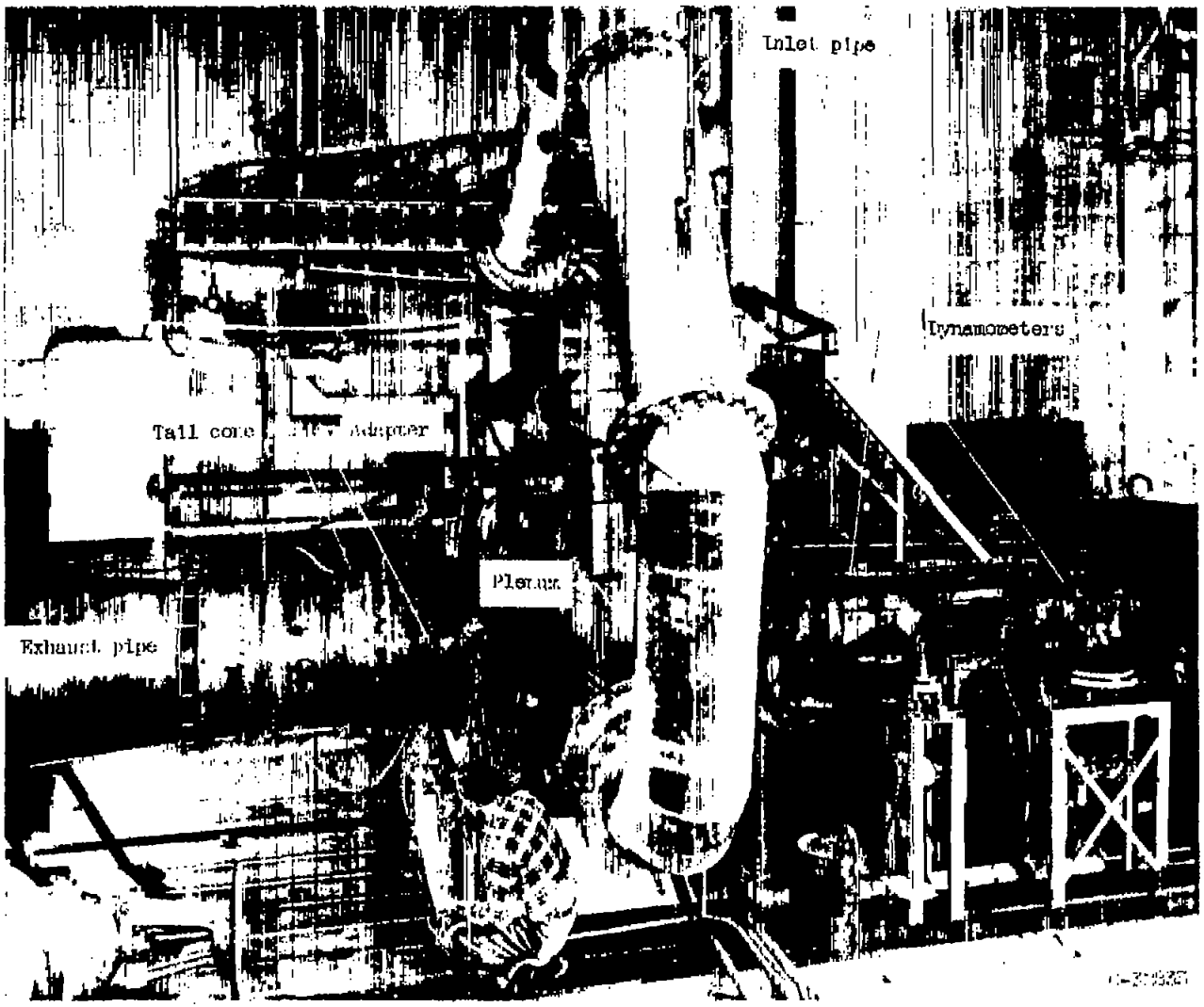

Figure 1. - Setup for investigation of performance of J73 turbine.

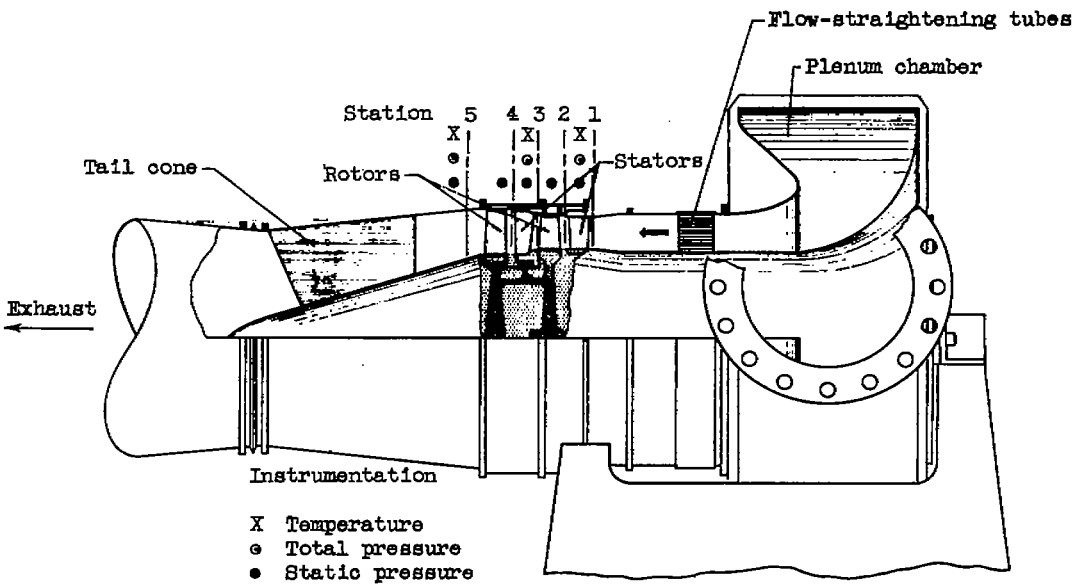

(a) Two-stage turbine.

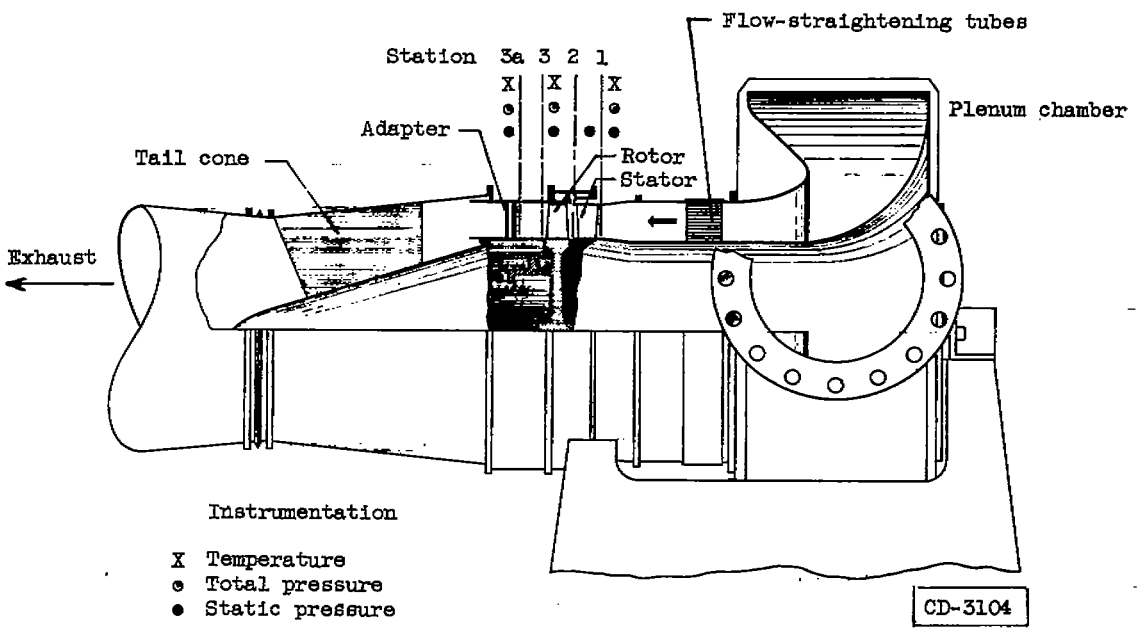

(b) First stage of turbine.

Figure 2. - Schematic diagrams of J73 turbine assemblies showing instrumentation.

[redacted]

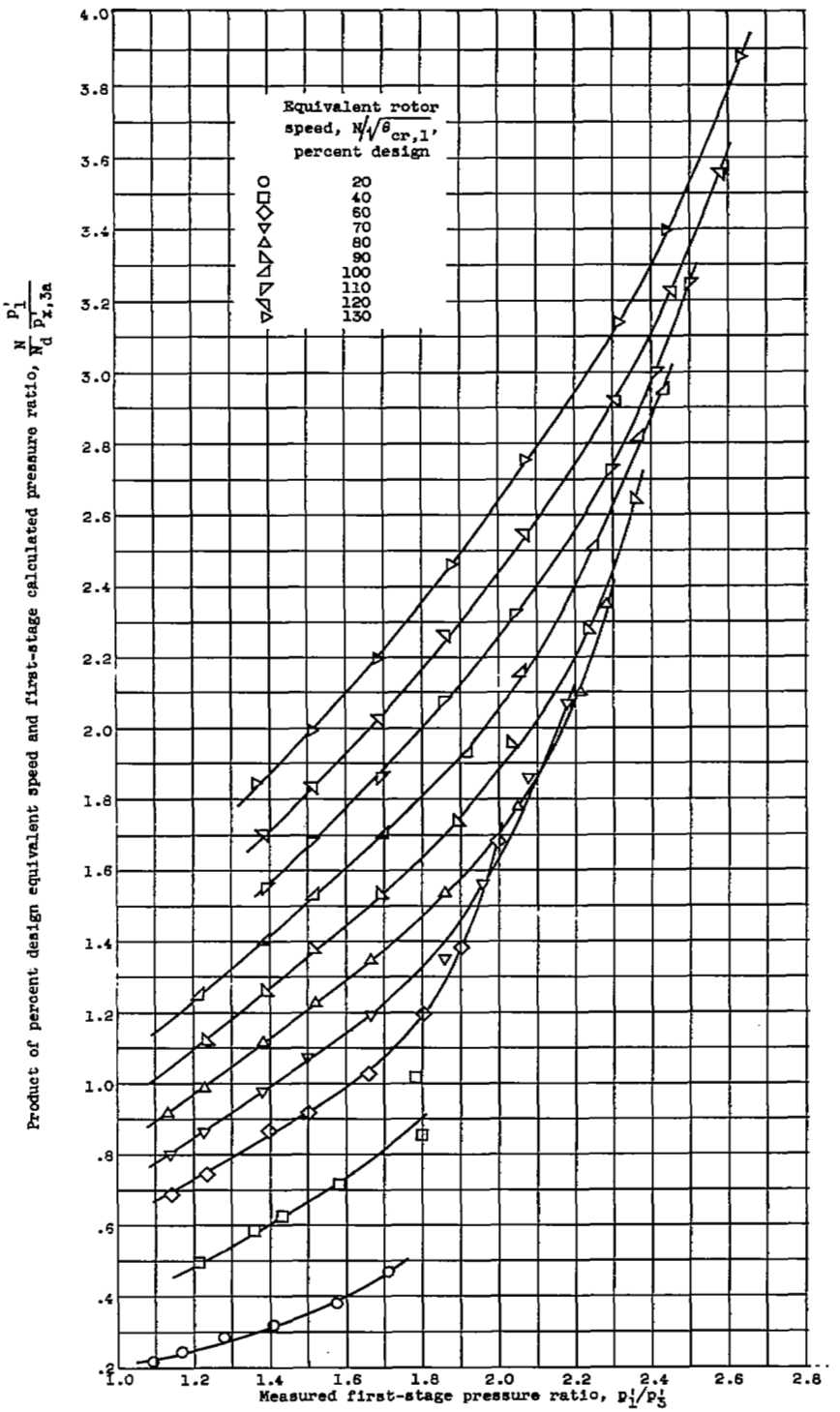

(a) Relation of calculated and measured pressure ratios.

Figure 3. - Correlation data for J73 first-stage turbine.

[redacted]

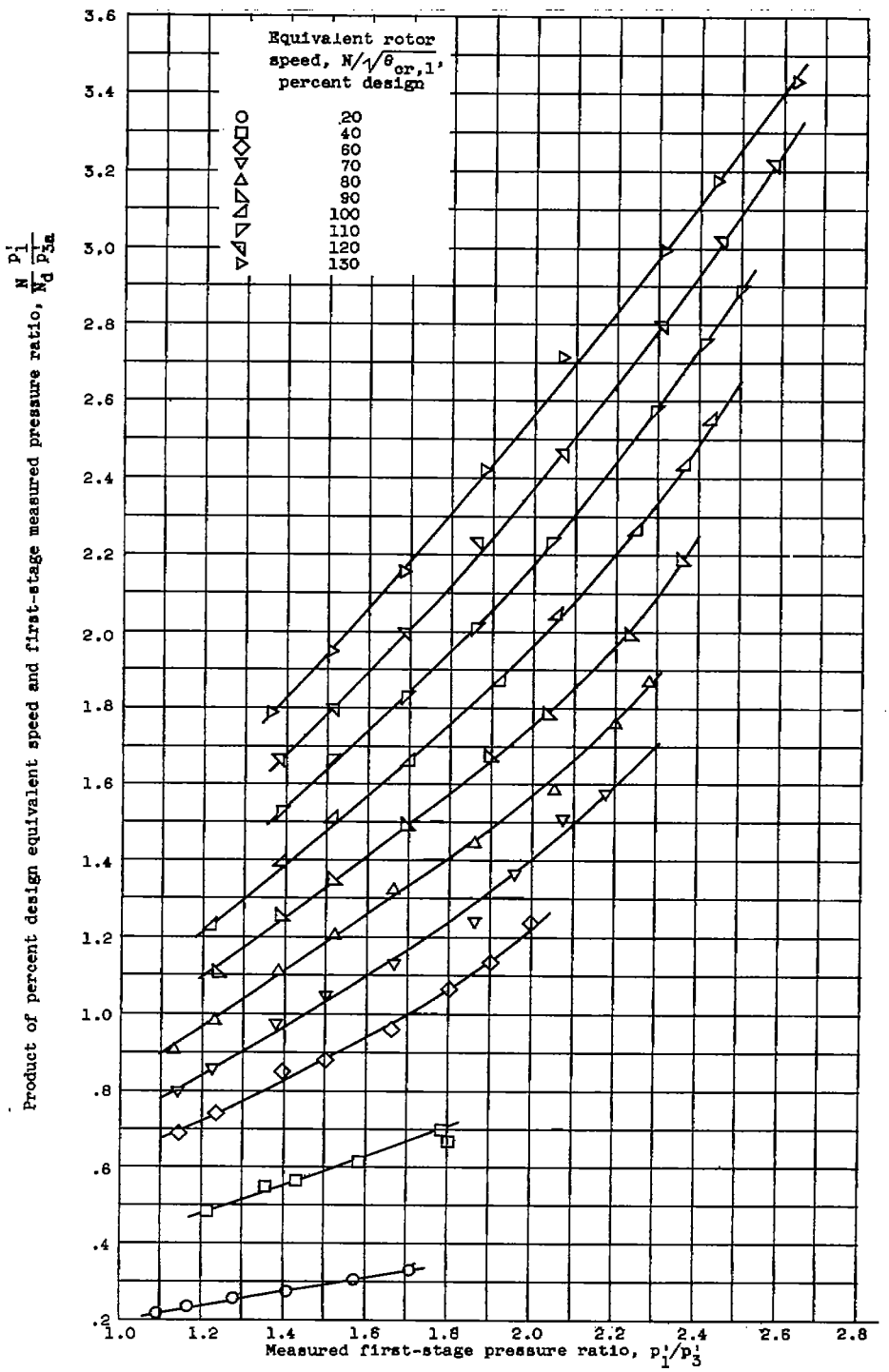

(b) Relation of measured pressure ratios at stations 3 and 3a.

Figure 3. - Continued. Correlation data for J73 first-stage turbine.

[redacted]

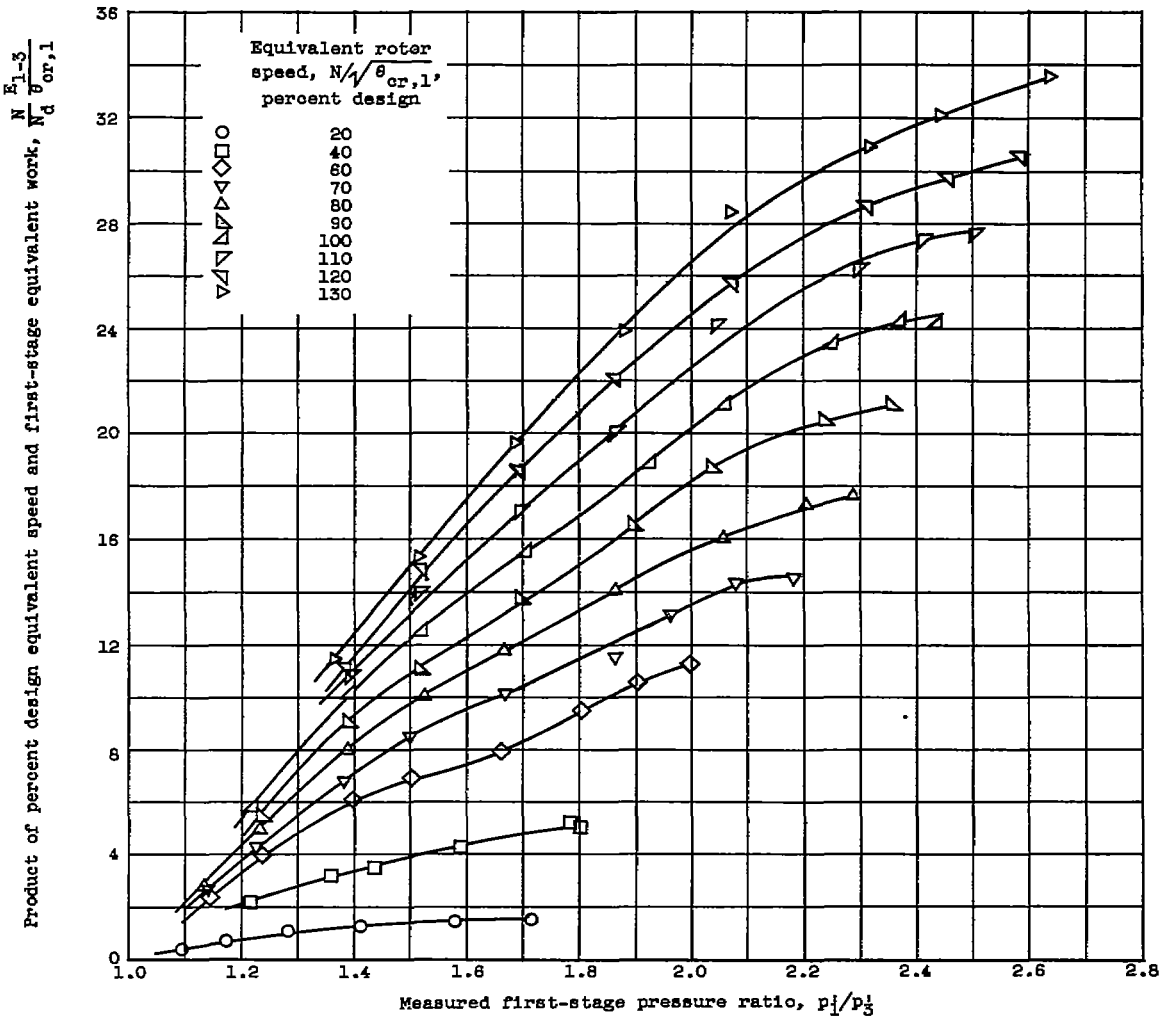

(c) Relation of equivalent work and measured pressure ratio.

Figure 3. - Concluded. Correlation data for J73 first-stage turbine.

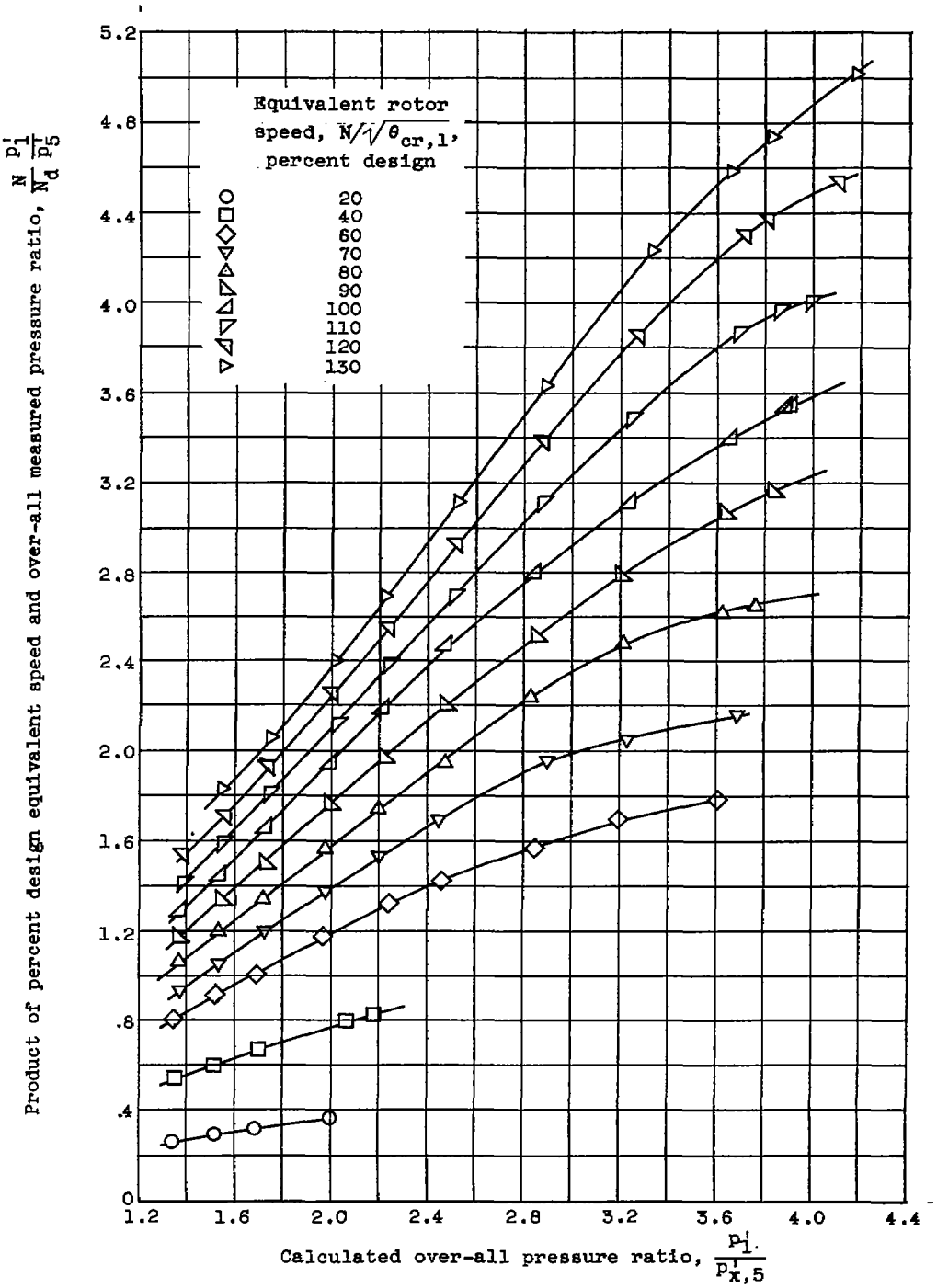

(a) Relation of calculated and measured pressure ratios.

Figure 4. - Correlation data for J73 two-stage turbine.

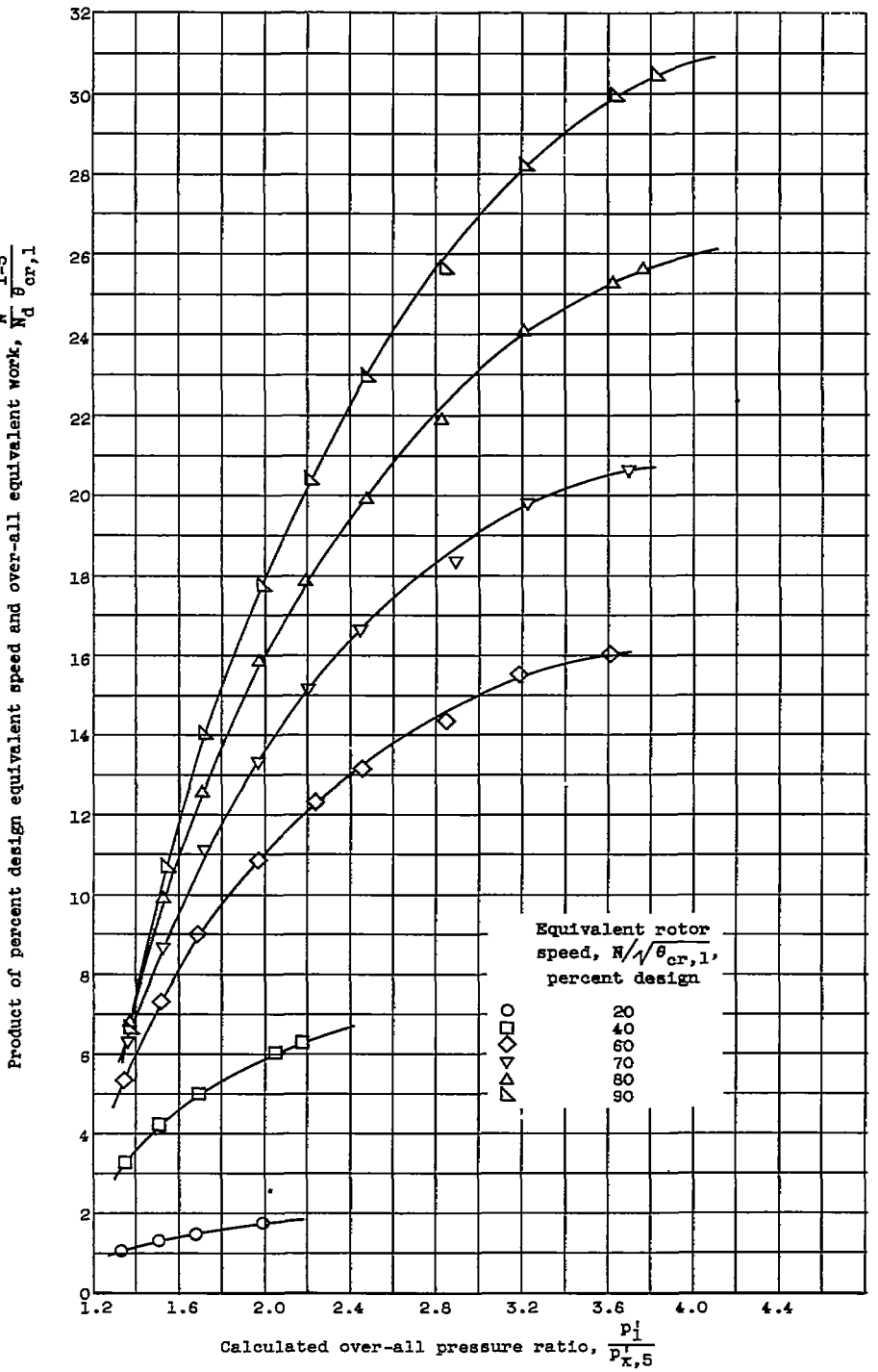

(b) Relation of equivalent work and calculated pressure ratio for equivalent speeds from 20 to 90 percent of design.

Figure 4. - Continued. Correlation data for J73 two-stage turbine.

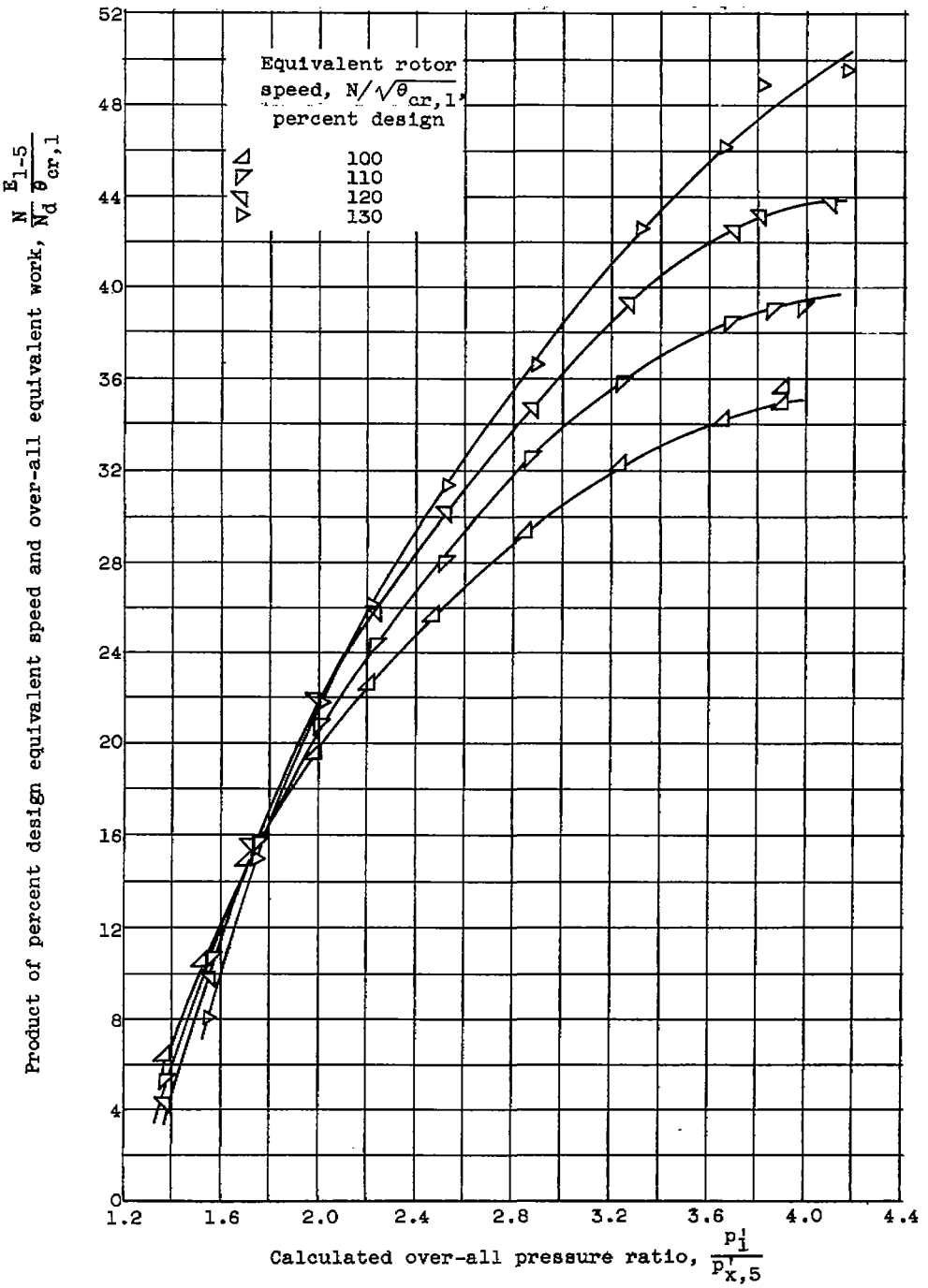

(c) Relation of equivalent work and calculated pressure ratio for equivalent speeds from 100 to 130 percent of design.

Figure 4. - Concluded. Correlation data for J73 two-stage turbine.

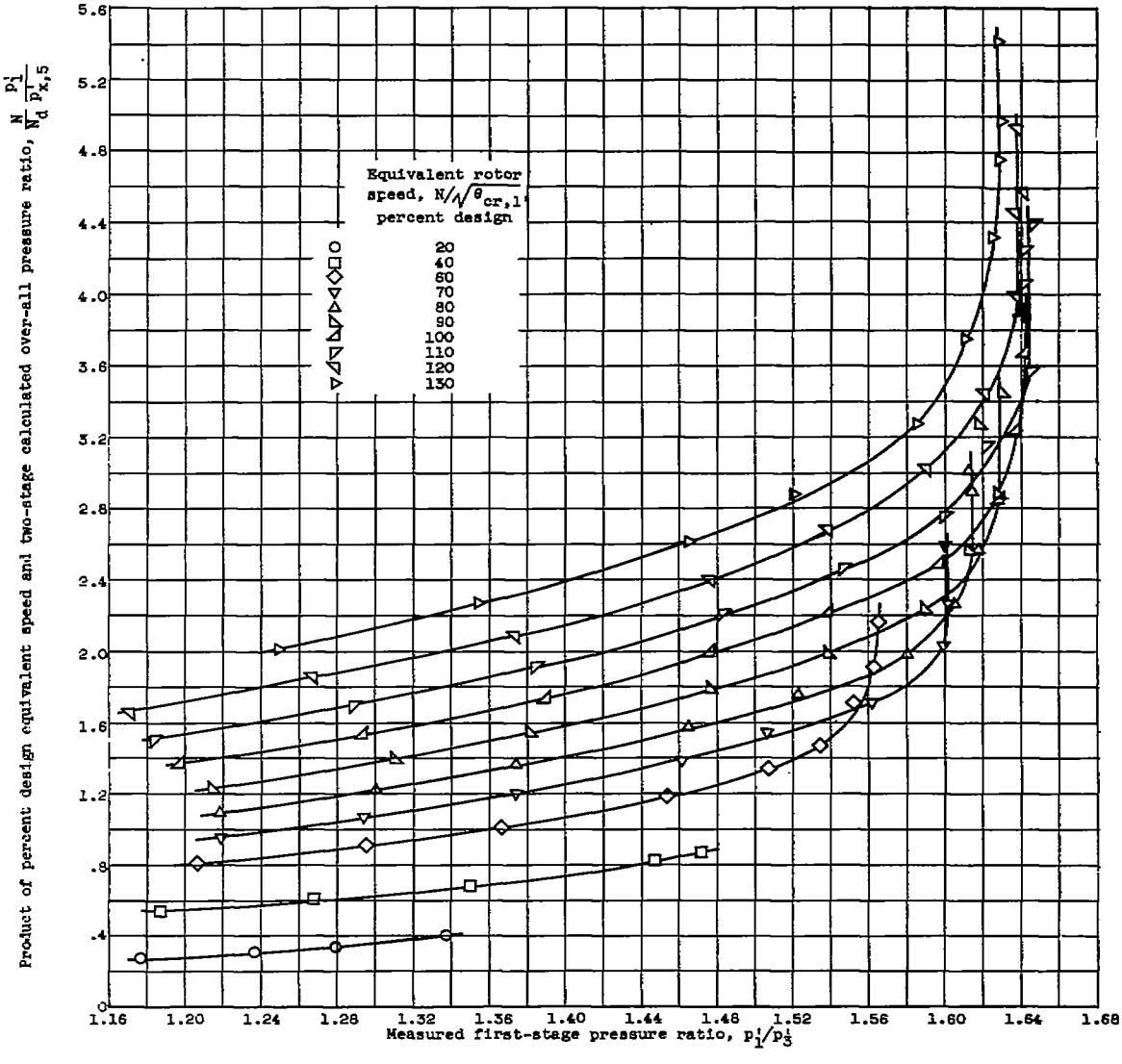

Figure 5. - Correlation curves indicating variation of calculated over-all pressure ratio with measured first-stage pressure ratio for J75 two-stage turbine.

[redacted]

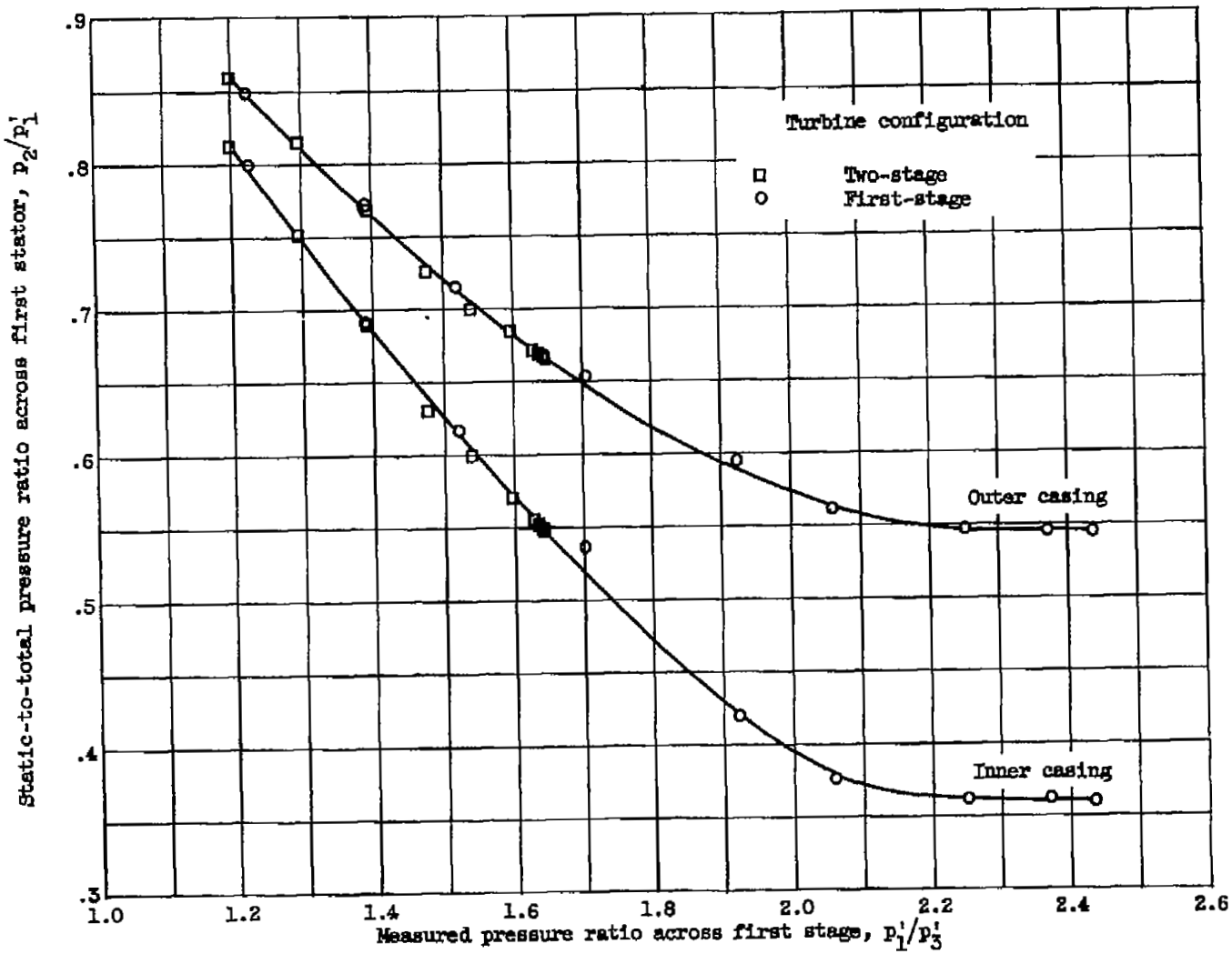

Figure 6. - Variation of static-to-total pressure ratio across first stator with measured total-pressure ratio across first stage for standard-bladed turbines at design speed.

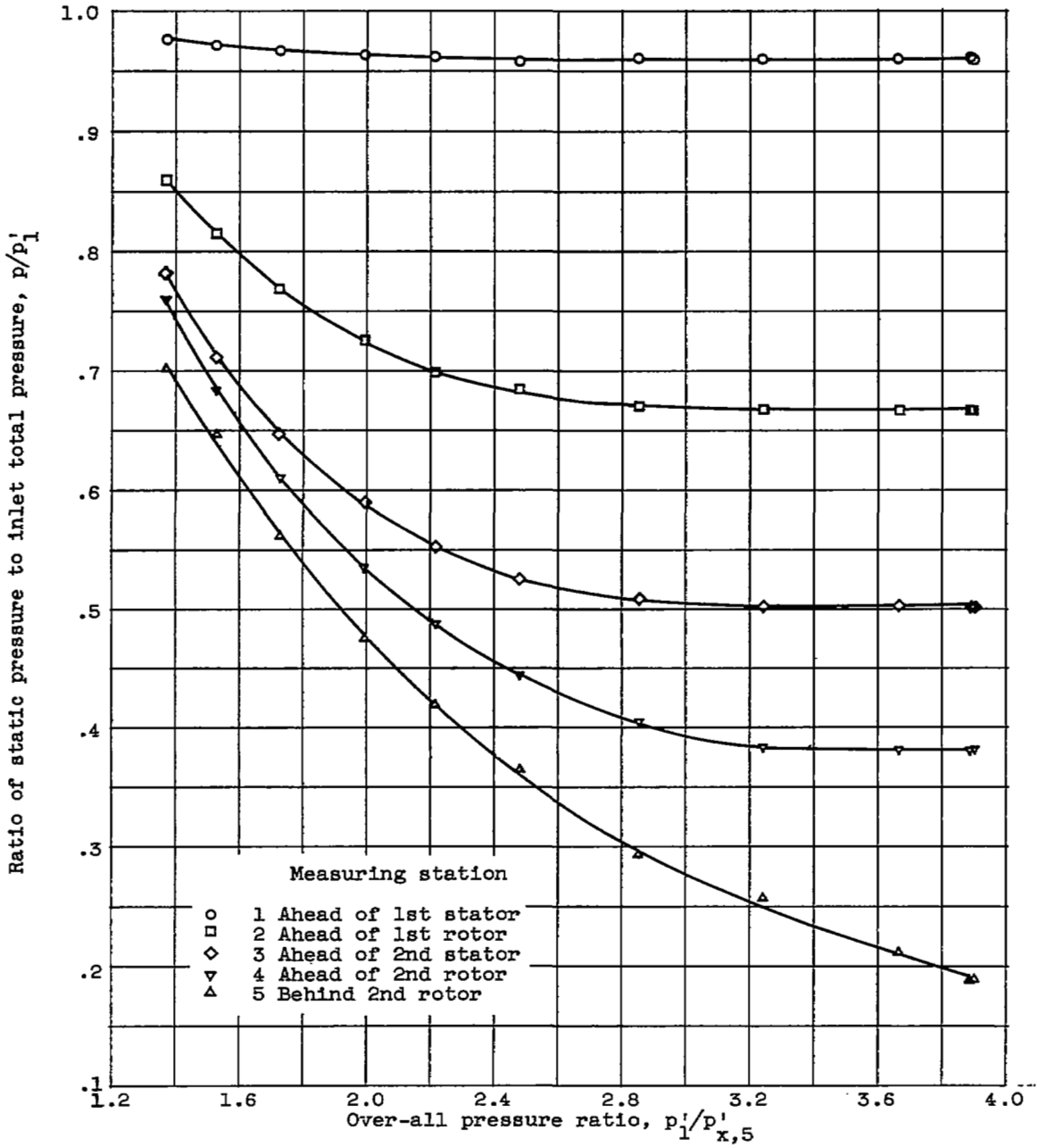

(a) Static pressures at outer casing.

Figure 7. - Variation of ratio of static pressure to inlet total pressure with over-all pressure ratio at different measuring stations for two-stage J73 turbine with standard rotor blading at design speed.

[redacted]

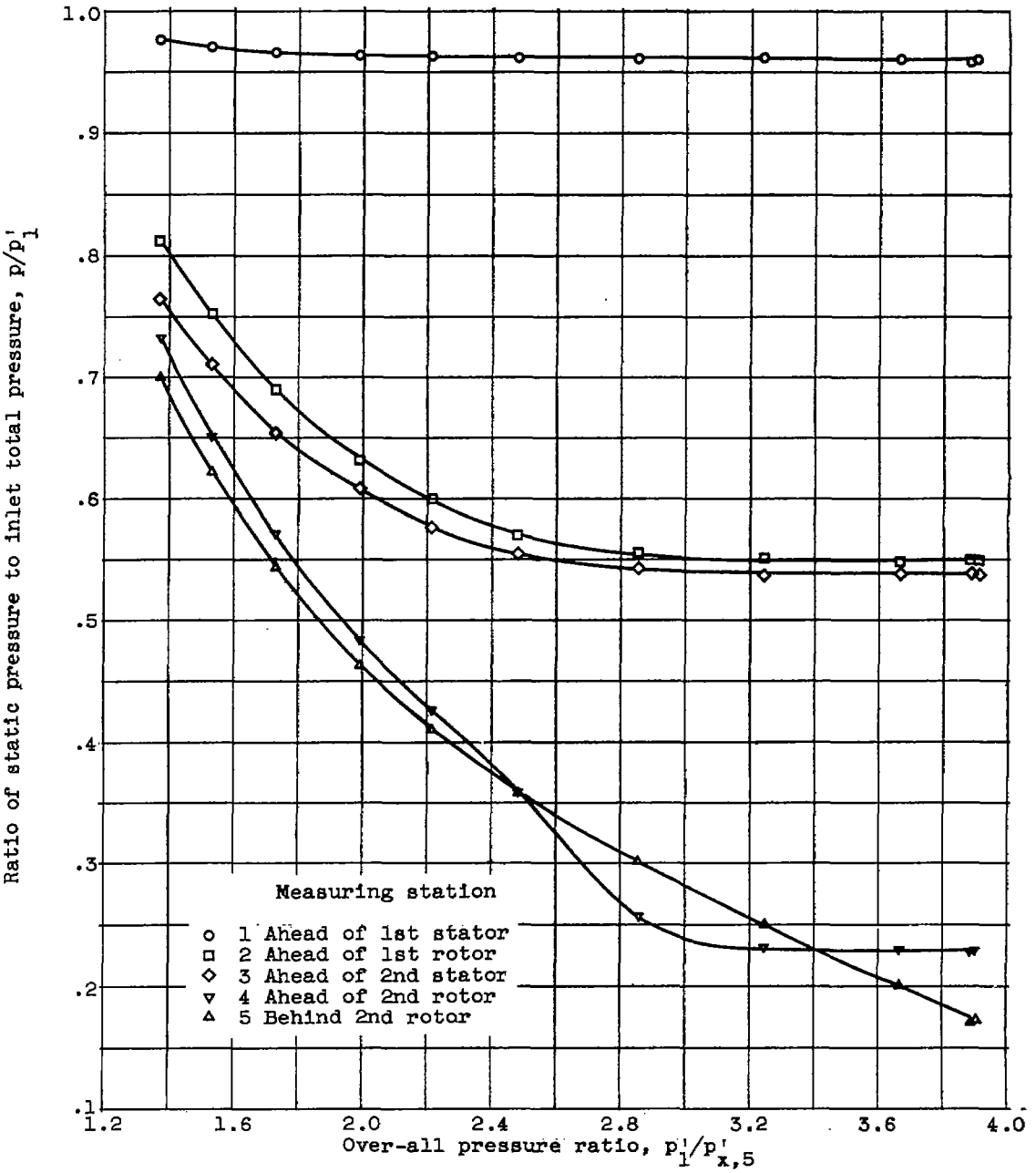

(b) Static pressures at inner casing.

Figure 7. - Concluded. Variation of ratio of static pressure to inlet total pressure with over-all pressure ratio at different measuring stations for two-stage J73 turbine with standard rotor blading at design speed.

[redacted]

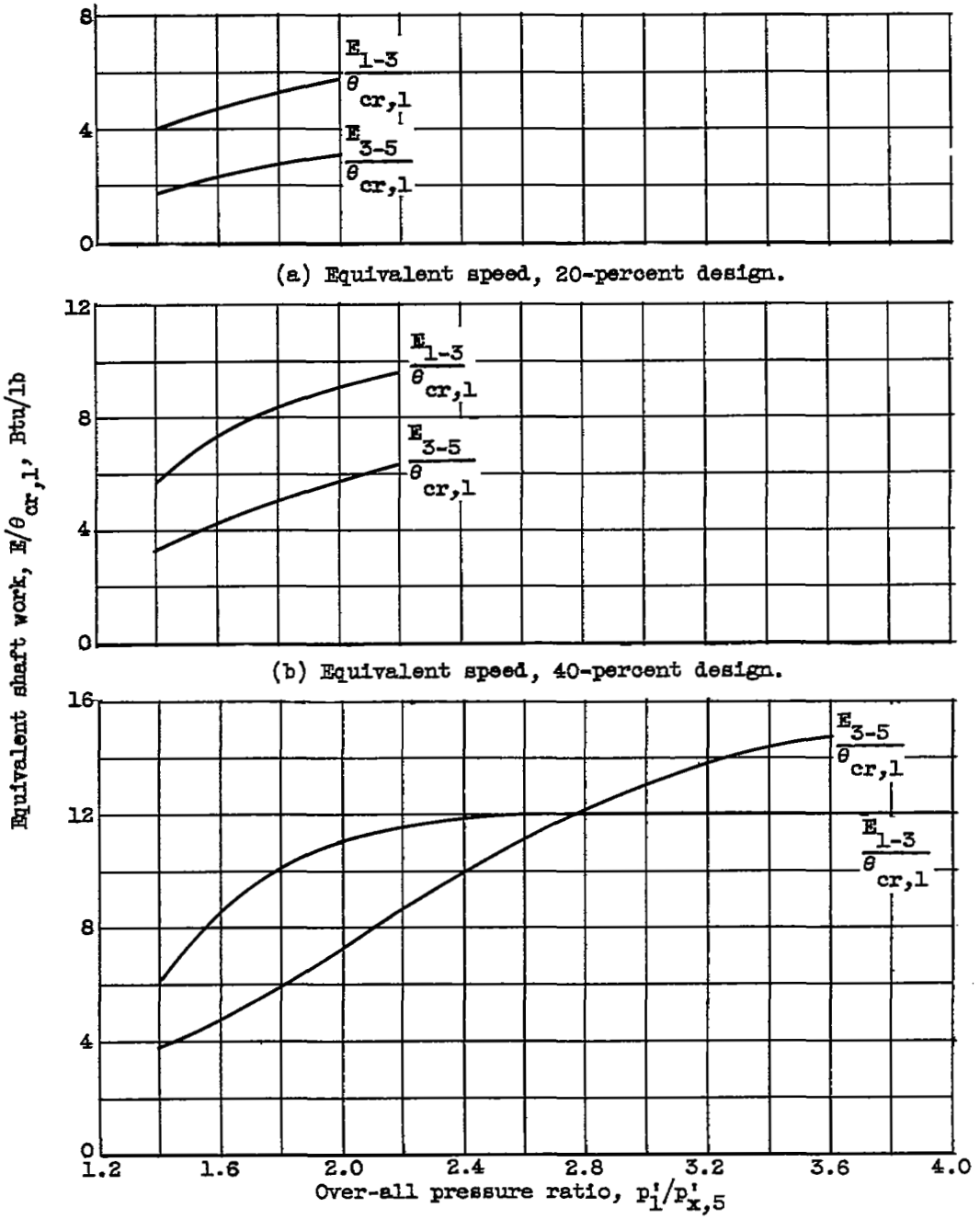

(a) Equivalent speed, 20-percent design.

(b) Equivalent speed, 40-percent design.

(c) Equivalent speed, 60-percent design.

Figure 8. - Variation of stage equivalent shaft work with turbine speed and over-all pressure ratio for J73 two-stage turbine.

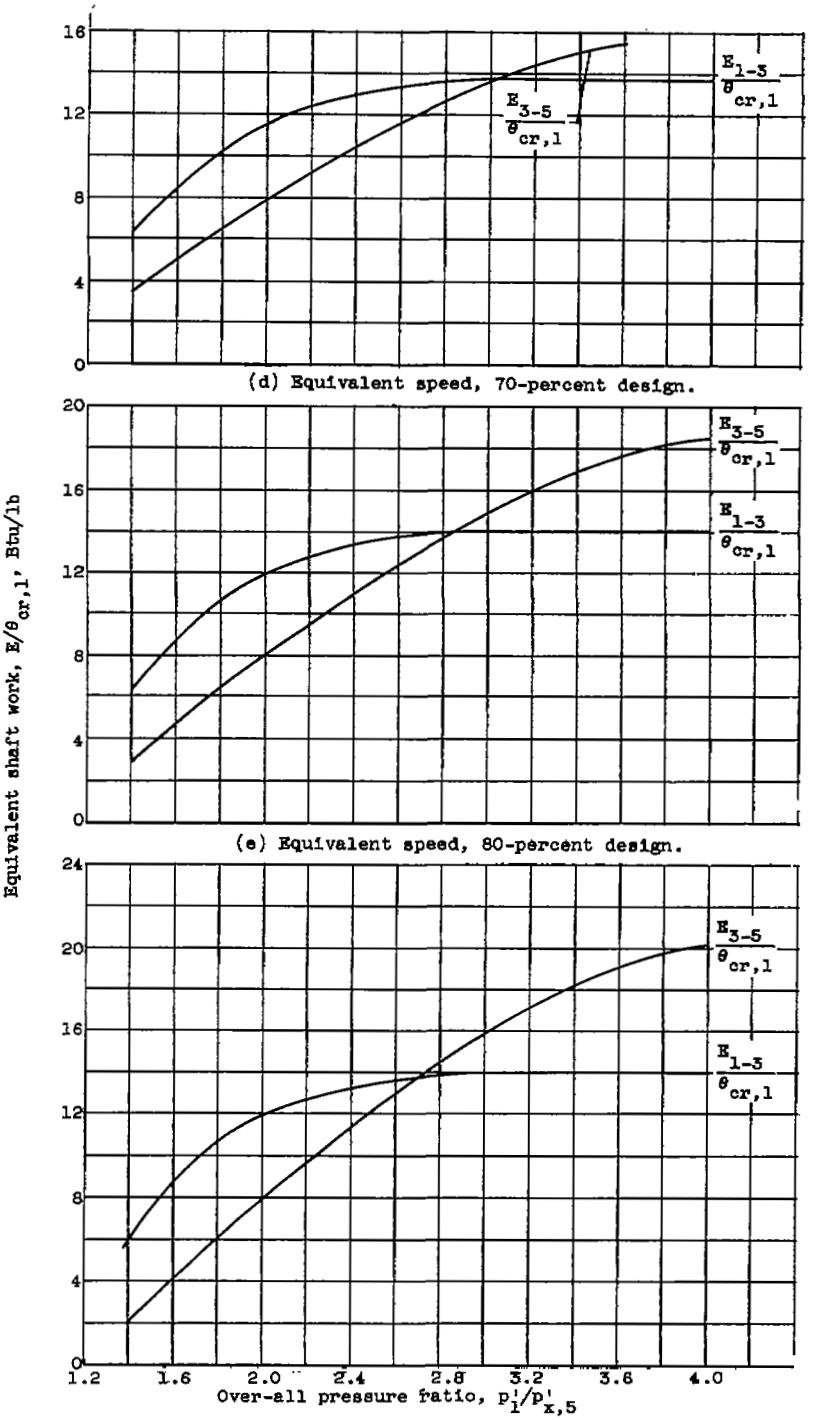

(d) Equivalent speed, 70-percent design.

(e) Equivalent speed, 80-percent design.

(f) Equivalent speed, 90-percent design.

Figure 8. - Continued. Variation of stage equivalent shaft work with turbine speed and over-all pressure ratio for J73 two-stage turbine.

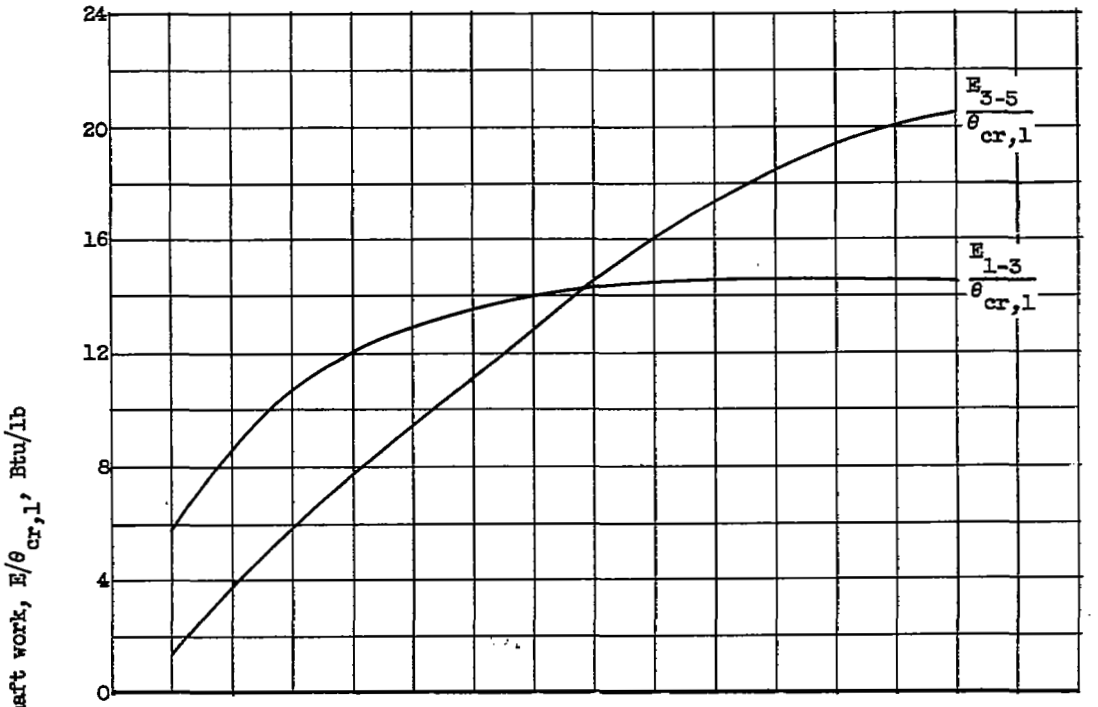

(g) Equivalent speed, 100-percent design.

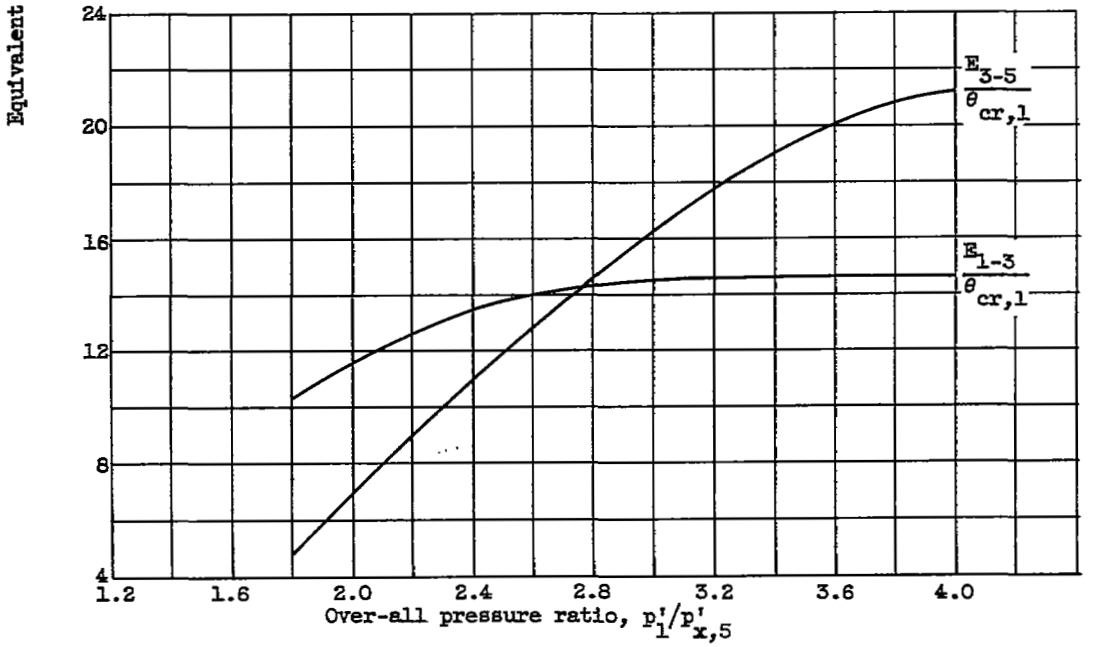

(h) Equivalent speed, 110-percent design.

Figure 8. - Continued. Variation of stage equivalent shaft work with turbine speed and over-all pressure ratio for J73 two-stage turbine.

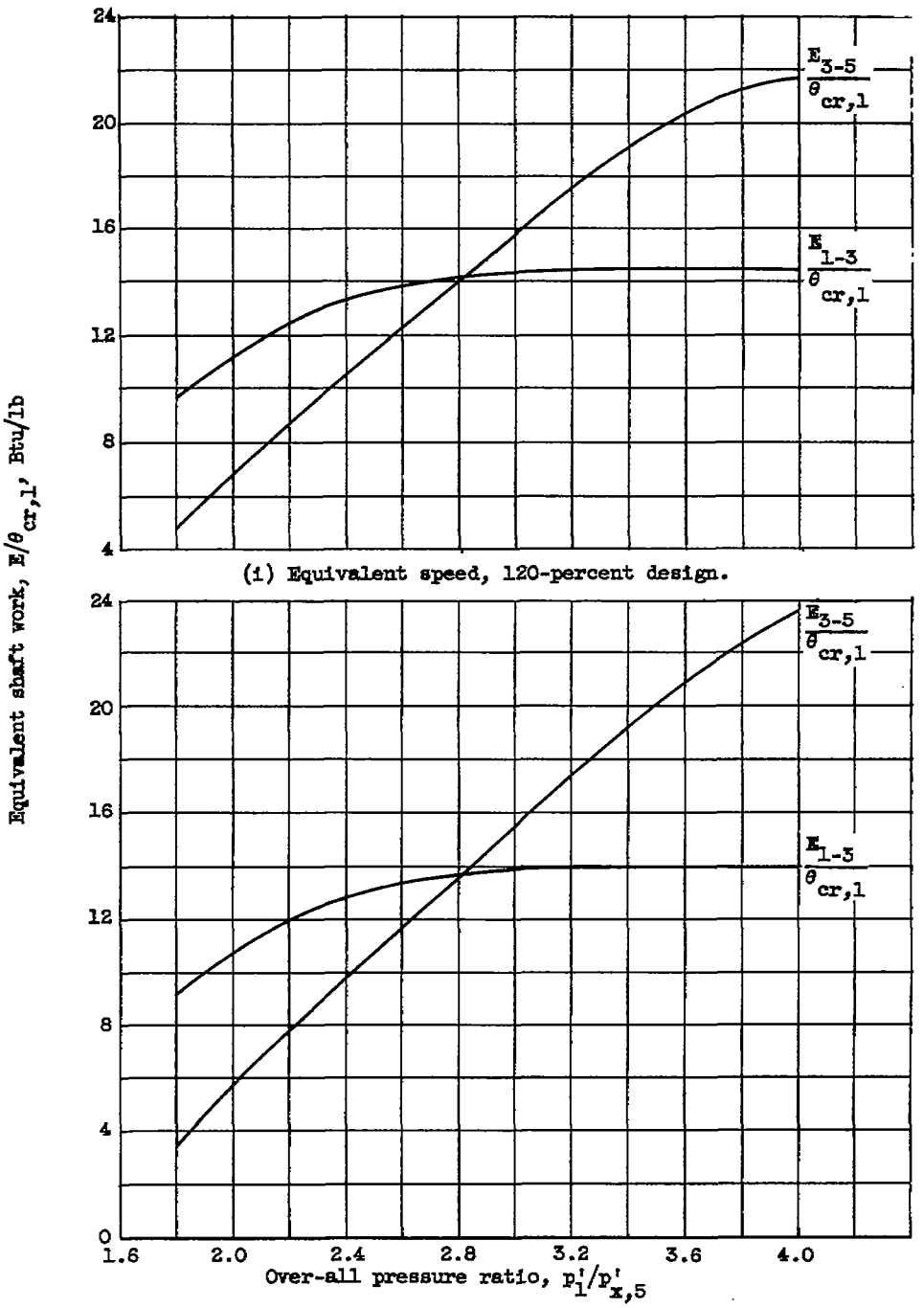

(i) Equivalent speed, 120-percent design.

(j) Equivalent speed, 130-percent design.

Figure 8. - Concluded. Variation of stage equivalent shaft work with turbine speed and over-all pressure ratio for J73 two-stage turbine.

[redacted]

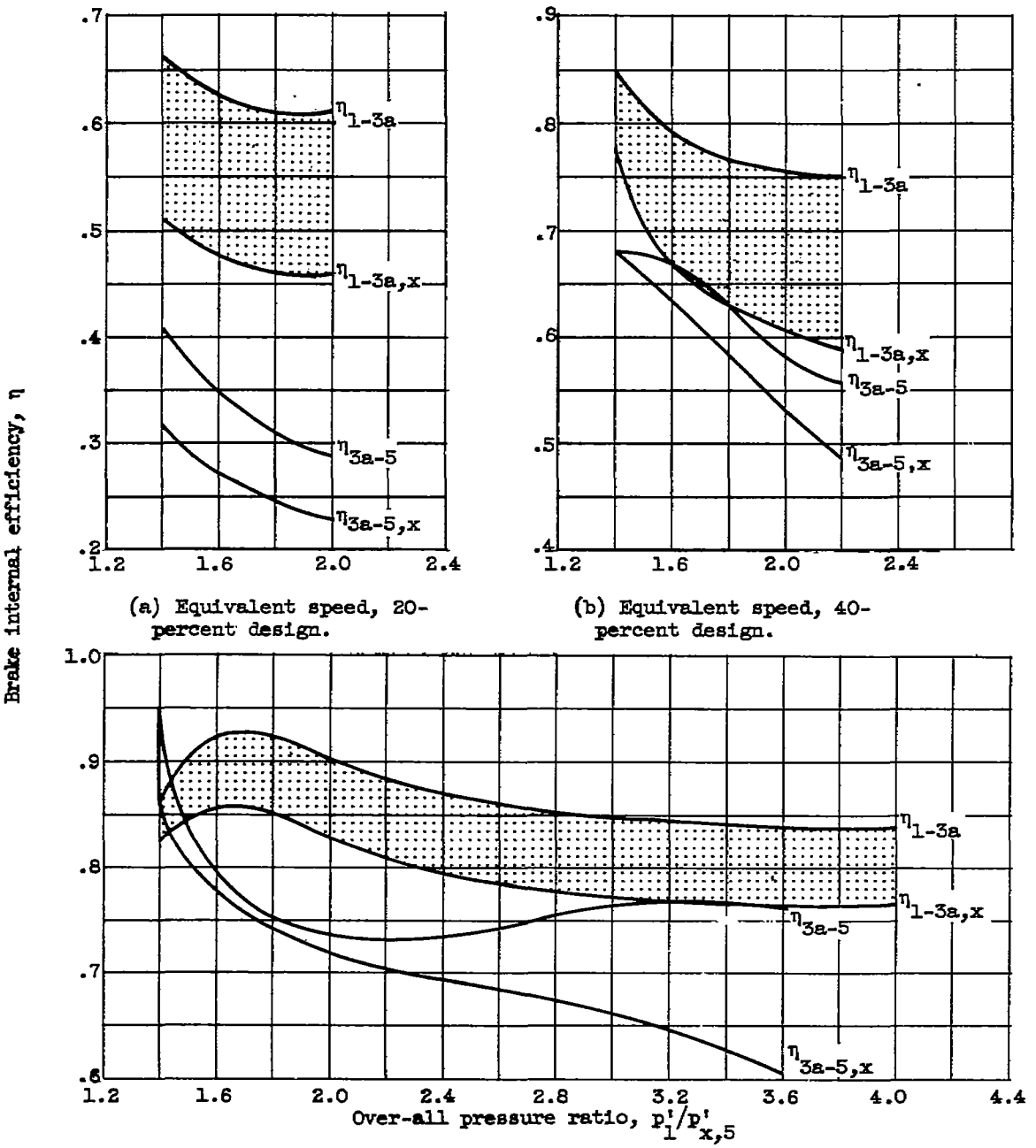

(a) Equivalent speed, 20-percent design.

(b) Equivalent speed, 40-percent design.

(c) Equivalent speed, 60-percent design.

Figure 9. - Variation of stage efficiencies with turbine speed and over-all pressure ratio for J73 two-stage turbine.

[redacted]

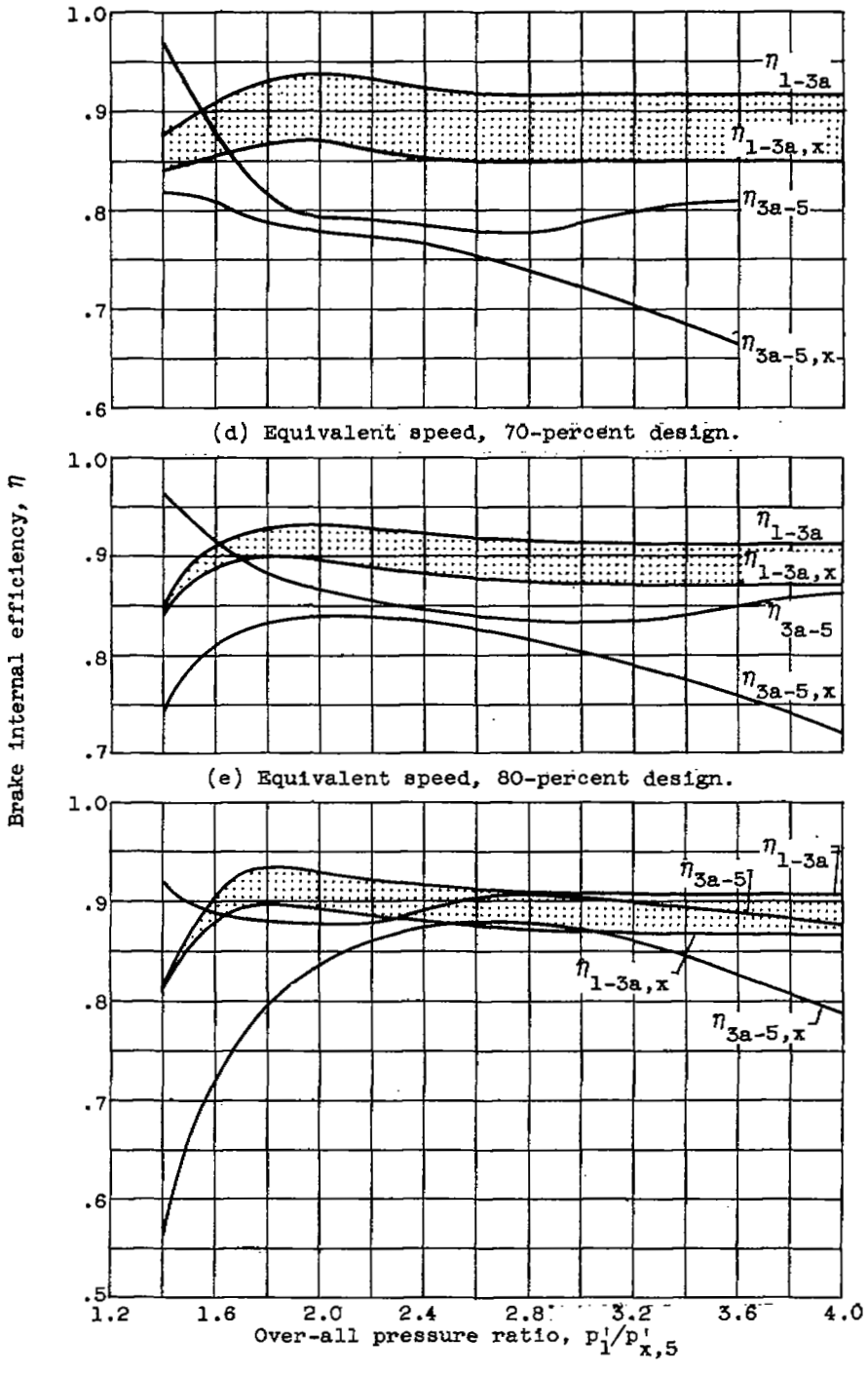

(d) Equivalent speed, 70-percent design.

(e) Equivalent speed, 80-percent design.

(f) Equivalent speed, 90-percent design.

Figure 9. - Continued. Variation of stage efficiencies with turbine speed and over-all pressure ratio for J73 two-stage turbine.

[redacted]

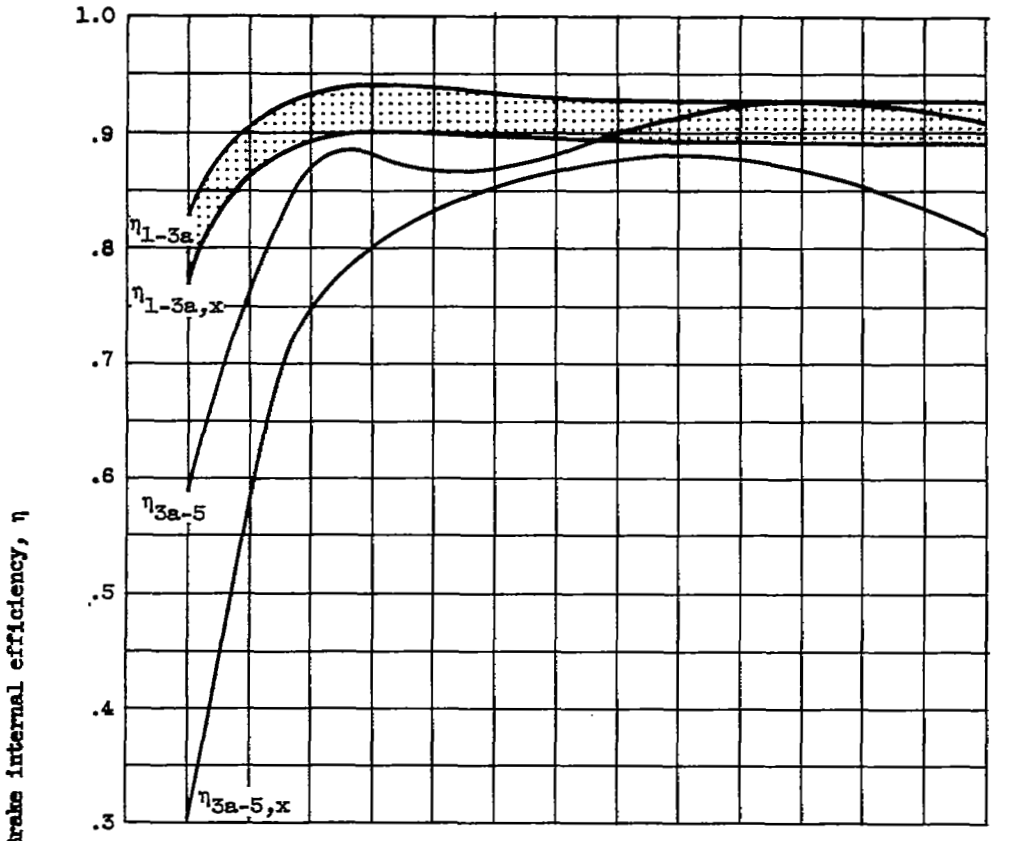

(g) Equivalent speed, 100-percent design.

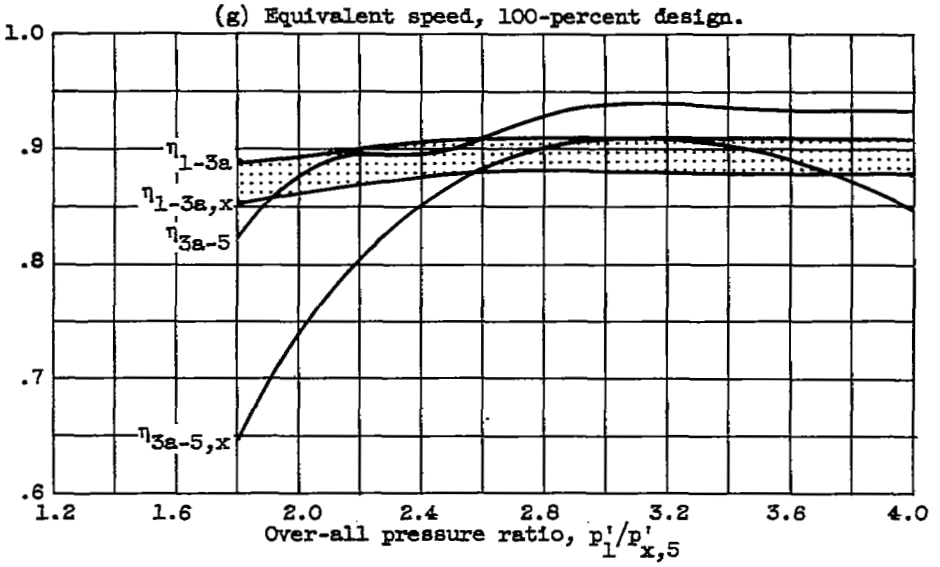

(h) Equivalent speed, 110-percent design.

Figure 9. - Continued. Variation of stage efficiencies with turbine speed and over-all pressure ratio for J73 two-stage turbine.

[redacted]

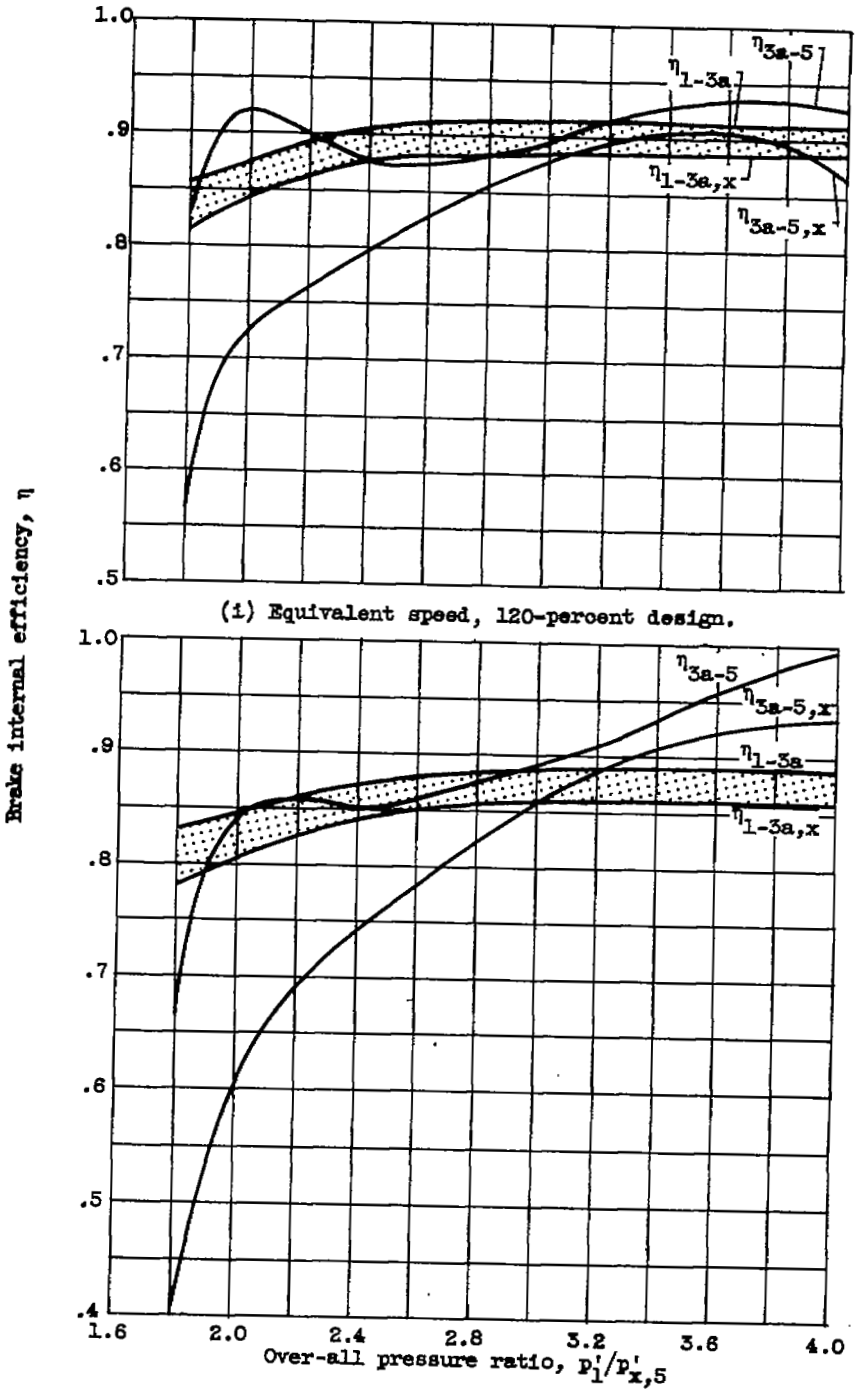

(i) Equivalent speed, 120-percent design.

(j) Equivalent speed, 130-percent design.

Figure 9. - Concluded. Variation of stage efficiencies with turbine speed and over-all pressure ratio for J73 two-stage turbine.

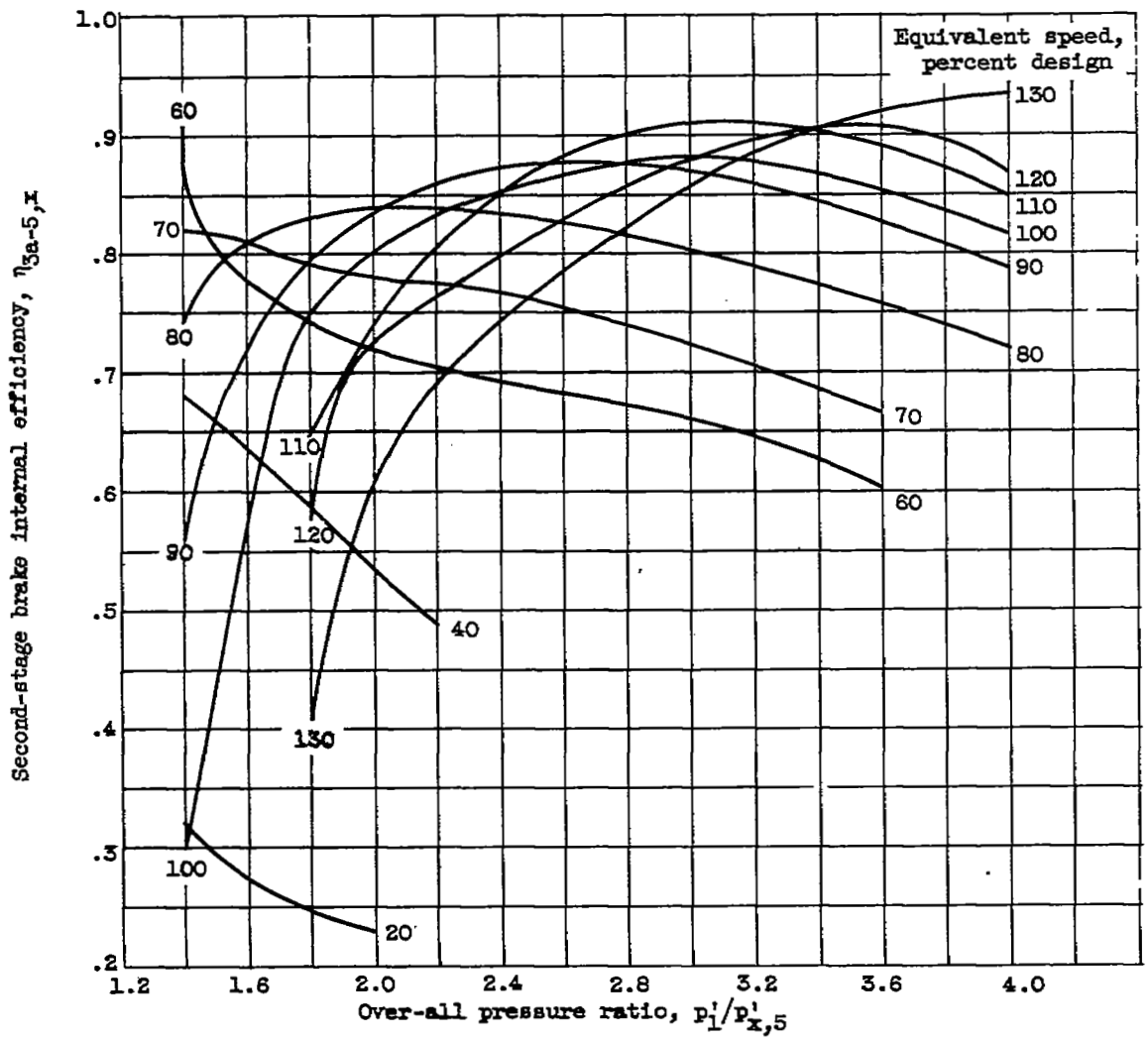

Figure 10. - Effect of turbine equivalent speed on second-stage efficiency.

[redacted]

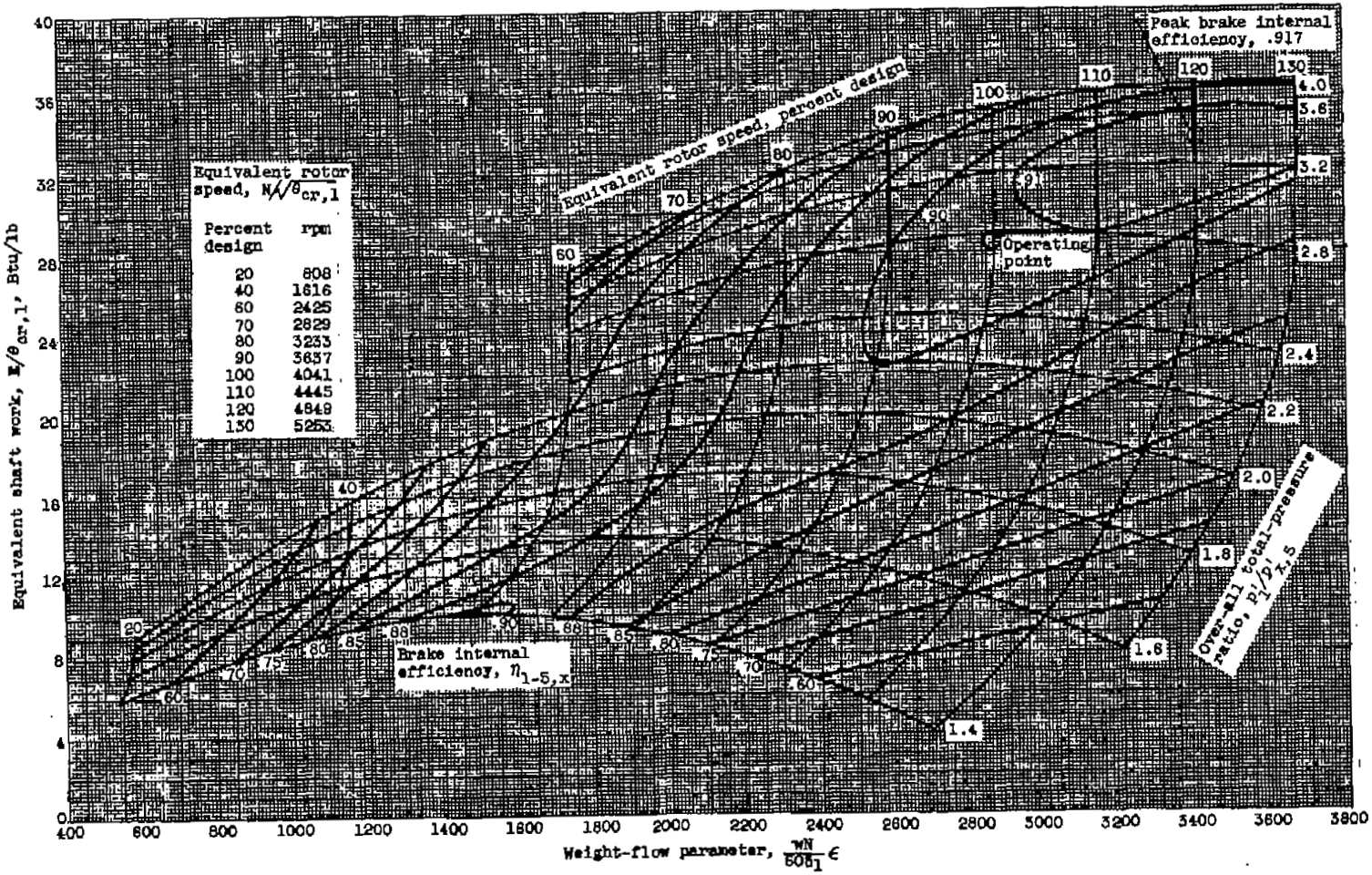

Figure 11. - Over-all performance of J73 two-stage turbine equipped with standard rotor blading. Turbine-inlet pressure, 55 inches of mercury absolute; turbine-inlet temperature, 700° R (ref. 2).

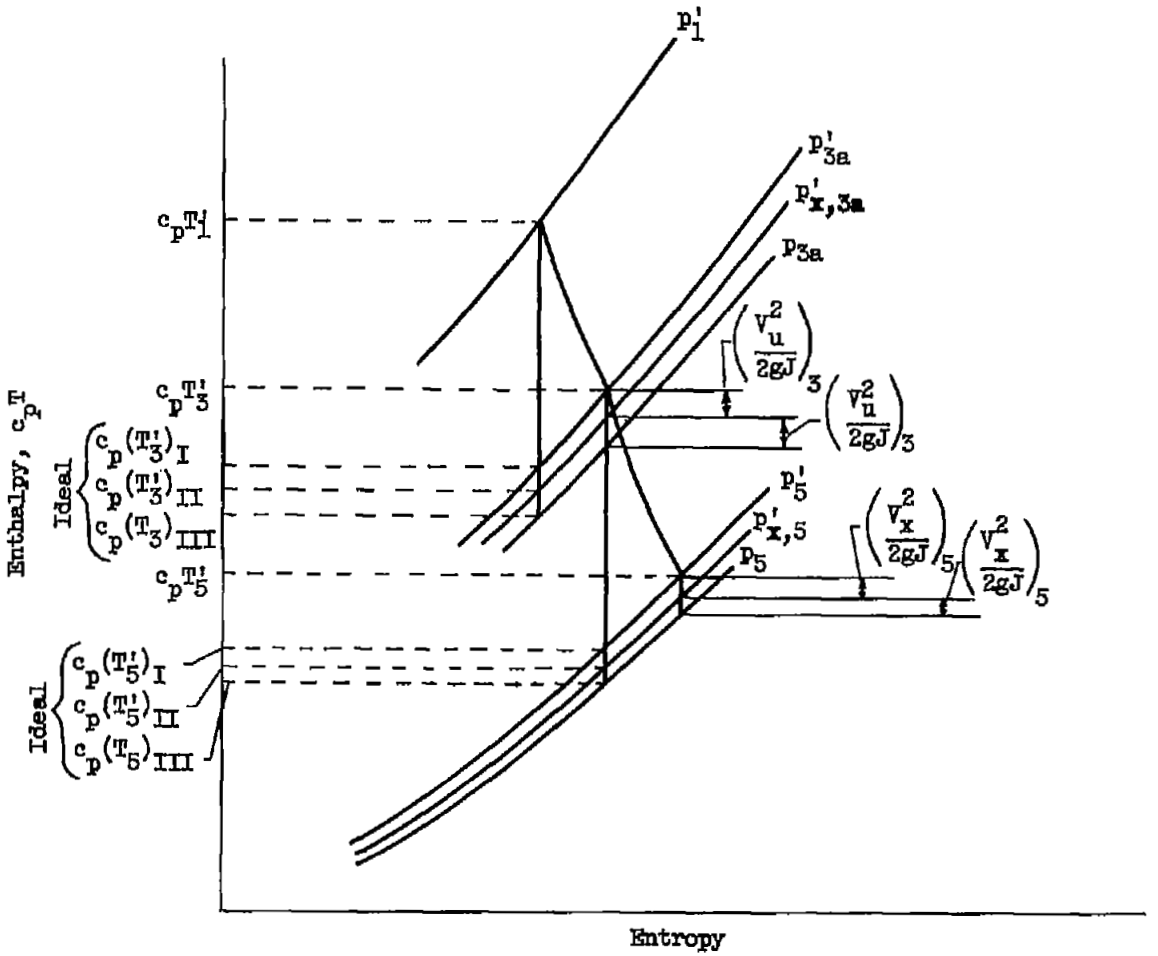

Figure 12. - Temperature-entropy diagram used to define stage efficiencies.